Lactoferrin perturbs lipid rafts and requires integrity of Pma1p-lipid rafts association to exert its antifungal activity against Saccharomyces cerevisiae

Cátia Santos-Pereira, María T Andrés, Susana R Chaves, José F Fierro, Hernâni Gerós, Stéphen Manon, Lígia R Rodrigues, Manuela Côrte-Real

Lactoferrin perturbs lipid rafts and requires integrity of Pma1p-lipid rafts association to exert its antifungal activity against *Saccharomyces cerevisiae*

Cátia Santos-Pereira[1,2], María T. Andrés[3], Susana R. Chaves[1], José F. Fierro[3], Hernâni Gerós[1], Stéphen Manon[4], Lígia R. Rodrigues[2], Manuela Côrte-Real[1]

[1] *Centre of Molecular and Environmental Biology (CBMA), Department of Biology, University of Minho, 4710-057 Braga, Portugal*

[2] *Centre of Biological Engineering (CEB), Department of Biological Engineering, University of Minho, 4710-057 Braga, Portugal*

[3] *Laboratory of Oral Microbiology, University Clinic of Dentistry (CLUO), and Department of Functional Biology (Microbiology), Faculty of Medicine, University of Oviedo, 33006 Oviedo, Asturias, Spain*

[4] *Institut de Biochimie et de Génétique Cellulaires, UMR5095, CNRS et Université de Bordeaux, CS61390, 1 Rue Camille Saint-Saëns, 33000 Bordeaux, France*

ABSTRACT

Lactoferrin (Lf) is a bioactive milk-derived protein with a remarkable wide-spectrum antifungal activity. To deepen our understanding of the molecular mechanisms underlying Lf cytotoxicity, the role of plasma membrane ergosterol- and sphingolipid-rich lipid rafts and their association with the proton pump Pma1p on Lf antifungal activity was explored. Pma1p was previously identified as a Lf-binding protein. Results showed that bovine Lf (bLf) perturbs sterol-rich lipid rafts distribution by inducing their intracellular accumulation. After a deep characterization of the phenotype of yeast mutant strains lacking lipid rafts-associated proteins or enzymes involved in the synthesis of ergosterol and sphingolipids, the normal composition of these membrane domains was found crucial for bLf-induced yeast cell death. Moreover, data showed that, when Pma1p-lipid rafts association is compromised in the Pma1-10 mutant and in the absence of the Pma1p-binding protein Ast1p, the bLf killing activity is impaired. Altogether, results showed that the perturbation of lipid rafts and the inhibition of both Pma1p and V-ATPase mediate the antifungal activity of bLf. Given that the combination of conventional antifungals with lipid rafts-disrupting compounds is suggested as a powerful antifungal approach, our data will help pave the way for the use of bLf alone or in combination for the treatment/eradication of clinically and agronomically relevant yeast pathogens/fungi.

INTRODUTION

Lactoferrin (Lf), a glycoprotein with ca. 80 kDa, is one of the most well-known milk bioactive proteins. Besides milk, it is present in many different biological fluids of mammalian species including mucosal surfaces, saliva and tears (Hao et al. 2019). Multiple biological activities have been attributed to this protein since it was first identified in bovine milk 80 years ago (Sorensen & Sorensen 1939), such as anticancer and antimicrobial, (Moreno-Expósito et al. 2018), including antifungal activity against different species of both yeasts and molds.

The mechanisms underlying the Lf antifungal activity described so far generally rely on its ability to sequester iron, to interact with the cell surface and to induce cell death (Fernandes & Carter 2017). In fact, we previously found that human Lf (hLf) induces an apoptotic-like cell death process in the yeasts *Candida albicans* (Andrés et al. 2008) and *Saccharomyces cerevisiae* (Acosta-Zaldívar et al. 2016), which is associated with nuclear chromatin condensation, increased production of reactive oxygen species and mitochondrial dysfunctions. Furthermore, we identified the plasma membrane proton pump Pma1p as a hLf-binding protein (Andrés et al. 2016). Pma1p is a P-type H+-ATPase that mediates proton extrusion powered by ATP hydrolysis to maintain pH homeostasis, ion balance and nutrient uptake in plant cells and fungi (Kane 2016). By binding and inhibiting Pma1p activity, hLf leads to increased intracellular ATP levels, perturbation of cytosolic pH and ion homeostasis and, consequently, lethal mitochondrial dysfunction (Andrés et al. 2016; Andrés et al. 2019).

Pma1p is known to be localized at specific nanodomains of the plasma membrane called lipid rafts (Bagnat et al. 2000; Mollinedo 2012). These are highly organized and tightly packed structures rich in ergosterol, sphingolipids and long saturated fatty acids that function as platforms for signalling and protein trafficking. They are generally identified as detergent-resistant membranes (DRMs) after cell fractioning with non-ionic detergents (Staubach & Hanisch 2011; Kodedová et al. 2019). Lipid rafts affect the mechanical properties of the plasma membrane and are involved in fungal pathogenicity and biofilm formation (Kodedová et al. 2019). Moreover, since lipid rafts are involved in the delivery of proteins to membranes such as multidrug resistance pumps, they have been implicated in drug resistance. Several antifungal peptides can target lipid rafts, affecting their integrity and the function of these pumps, which allows them to overcome drug resistance and to induce cell death (Pasrija et al. 2005; Kodedová et al. 2019). Combination of antifungal peptides targeting lipid rafts with

conventional antifungal drugs has thus been suggested as a powerful antifungal strategy (Rautenbach et al. 2016).

Different reports have supported the importance of lipid rafts for Pma1p functions. Indeed, lipid raft association is known to be crucial for proper surface targeting and Pma1p stability at the plasma membrane (Gong & Chang 2001). In accordance, disruption of lipid rafts leads to mistargeting of Pma1p to the vacuole (Bagnat et al. 2001). Synthesis of sphingolipids, which are abundant in lipid rafts, is also required for Pma1p oligomerization at the ER, targeting to the plasma membrane, and stability at the cell surface (Lee et al. 2002; Wang & Chang 2002). Given this interplay and interdependence between Pma1p and lipid rafts, and because Lf binds and inhibits Pma1p, in the present study we aimed to uncover the role of lipid rafts in Lf-induced cell death and to explore the Lf-Pma1p-lipid rafts axis.

Because human and bovine Lfs share a high degree of sequence identity (69%) (Pierce et al. 1991) and exhibit very similar structure (Steijns & van Hooijdonk 2000) and function/activity against fungi (Kuipers et al. 1999), bLf was chosen. Yeast mutant strains lacking lipid rafts-associated proteins or enzymes that mediate the synthesis of ergosterol and sphingolipids were used in this study as a model of lipid rafts perturbation. The Rvs161p (encoded by *RVS161/END6* gene) is a protein known to be localized in lipid rafts/detergent resistant membranes (DRMs) and to be involved, among others, in actin cytoskeleton polarization, cell polarity and endocytosis (Balguerie et al. 2002). The *ERG6* gene encodes the sterol C-24 methyltransferase, an enzyme that acts in the final steps of ergosterol biosynthesis by converting zymosterol to fecosterol (Fig. 1A). Therefore, *erg6*Δ mutants accumulate mainly zymosterol and cholesta-5,7,24-trienol instead of ergosterol (Munn et al. 1999). The other two genes under study are involved in sphingolipid metabolism. Sphingolipids are a multifunctional class of lipids greatly enriched in lipid rafts of eukaryotic cells, and are important for the formation of these structures (Martinez-Montanes et al. 2016). *LAC1* encodes a component of ceramide synthase and is involved in *de novo* synthesis of ceramide by N-acylation of sphingoid bases (Fig. 1B) (Cowart & Obeid 2007). The *ISC1* gene encodes the mitochondrial inositol phosphosphingolipid phospholipase C, which is involved in the synthesis of ceramide by hydrolysis of complex sphingolipids (Fig. 2B) (Cowart & Obeid 2007).

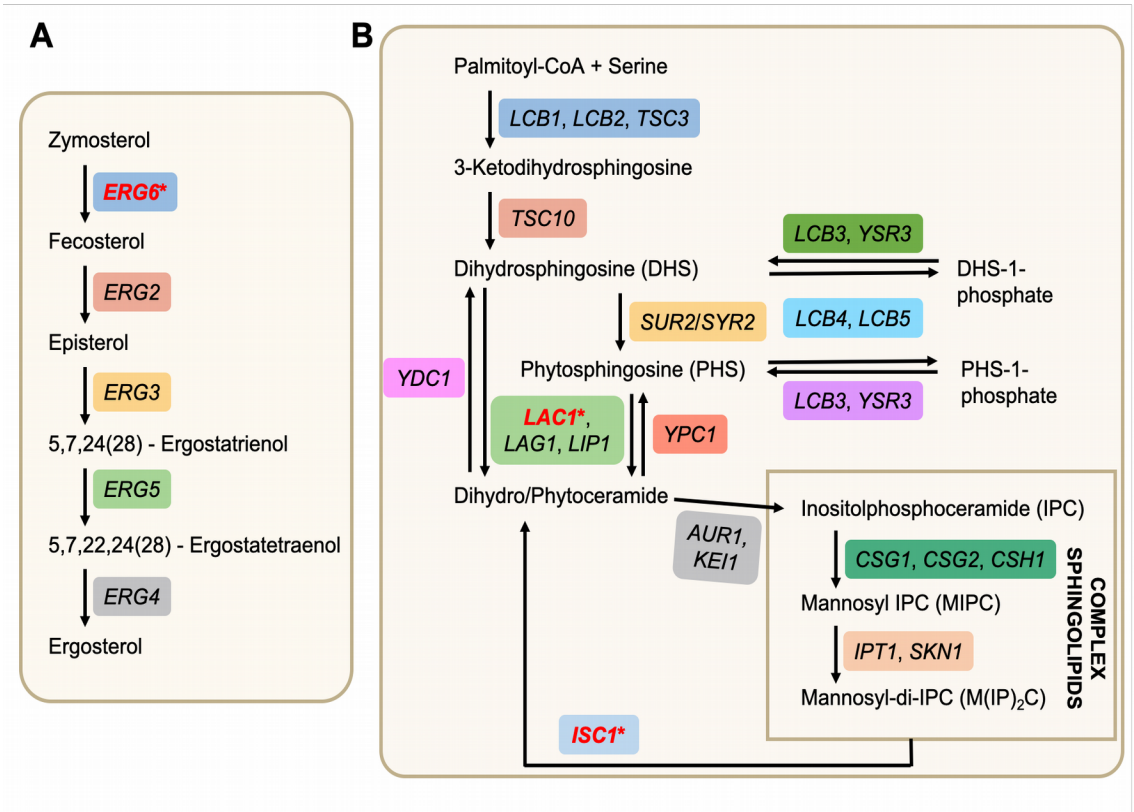

Figure 1 | Ergosterol (A) and sphingolipid (B) biosynthetic pathways in *Saccharomyces cerevisiae*. For ergosterol, only the last steps of the biosynthetic pathway are represented. The genes that were deleted to construct the mutant strains used in this work are marked in red with an asterisk (*).

RESULTS

1. bLf induces intracellular accumulation of sterol-rich lipid rafts in yeast cells

In order to ascertain whether sterol-rich lipid rafts play a role in Lf-induced cytotoxicity in yeast, we first assessed their cellular distribution upon Lf treatment. Since sterols are major lipid rafts components, we monitored cellular ergosterol localization using filipin staining after 90 min exposure to 250-500 µg/ml of bLf, which induces loss of cell viability of ca. 70% - 98%, respectively (Fig. 2A). As shown in Fig. 1B, the characteristic punctuated pattern of the lipid rafts at the plasma membrane (head arrows) is observed in control cells, while intracellular spots of filipin staining (arrows) are visible in bLf-treated cells. To confirm that this intracellular staining indeed corresponds to an alteration in ergosterol distribution, yeast cells were treated with methyl-β-cyclodextrin (MβCD), a sterol chelator known to disrupt lipid rafts by depleting ergosterol from membranes (Siafakas et al. 2006). Treatment with this compound induced a similar intracellular filipin-staining pattern as bLf. These results indicate

that bLf perturbs the normal sterol-rich lipid rafts distribution pattern by causing their intracellular accumulation.

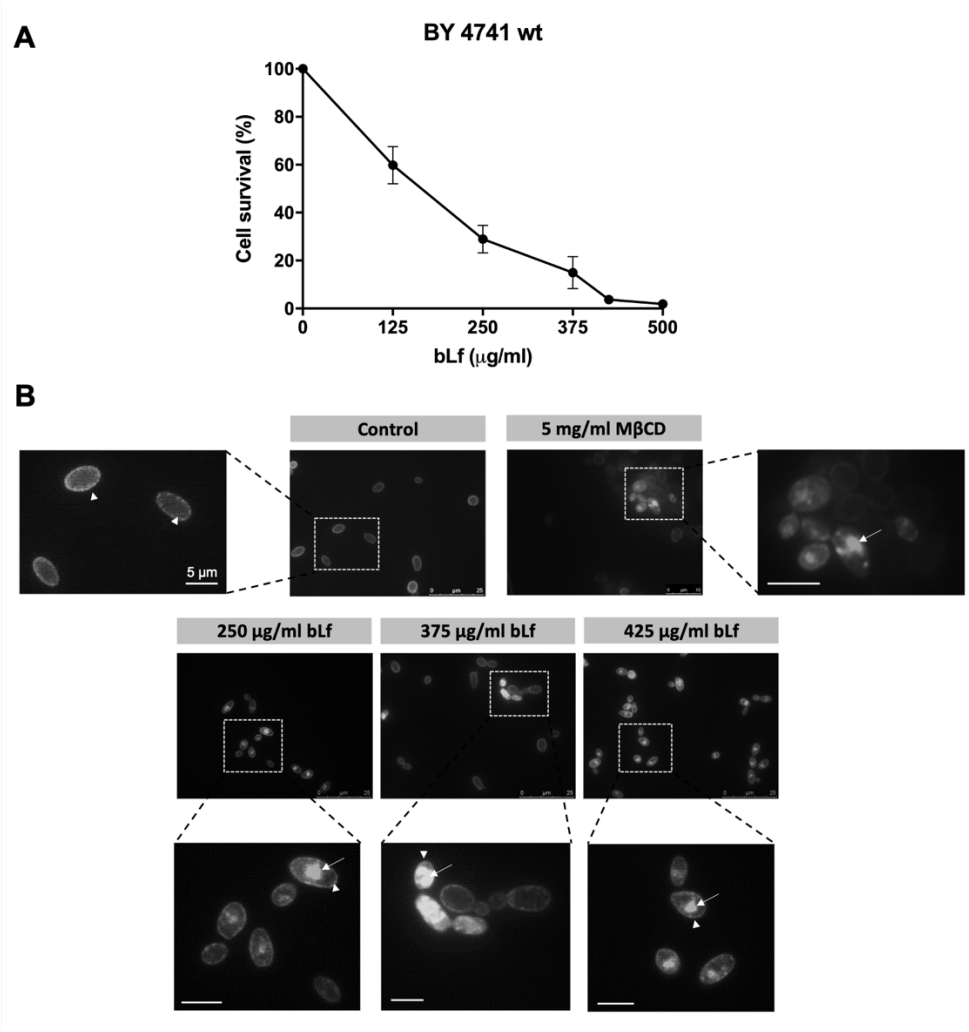

Figure 2 | Effect of bLf on the localization of sterol-rich lipid rafts in *S. cerevisiae* BY4741 cells. Cells were incubated in the absence or presence of increasing concentrations of bLf (125-500 μg/ml) for 90 min at 30˚C in Tris-HCl 10 mM, pH 7.4 buffer. **(A)** Cell survival was assessed by counting colony forming units. **(B)** For lipid rafts visualization, cells were stained in the dark with 0.1 mg/ml filipin immediately before visualization under the microscope. As a positive control of lipid rafts disruption, cells were treated with 5 mg/ml methyl-β-cyclodextrin (MβCD) for 30 min. Representative fluorescence microscopy images of each condition are shown. Arrows: intracellular filipin staining. Head arrows: plasma membrane filipin staining. Bar: 5 μm.

2. Yeast mutants lacking lipid rafts-associated proteins or enzymes involved in the synthesis of the lipid rafts major components are more resistant to bLf-induced cytotoxicity

We next assessed the impact of perturbing lipid rafts using yeast mutants lacking proteins that are either present at lipid rafts or are involved in pathways that lead to the synthesis of their major lipid components, ergosterol and sphingolipids, namely *rvs161*Δ, *erg6*Δ, *lac1*Δ

and *isc1*Δ mutants. Results from cell survival assays showed that absence of these proteins greatly increases the resistance of the mutant cells to bLf-induced cytotoxicity in comparison with the wild type strain (Fig. 3A). Remarkably, even at 500 µg/ml, which is highly toxic for the wild type strain (only about 2% cell survival), the mutants affected in sphingolipid metabolism exhibit ca. 23% of cell survival.

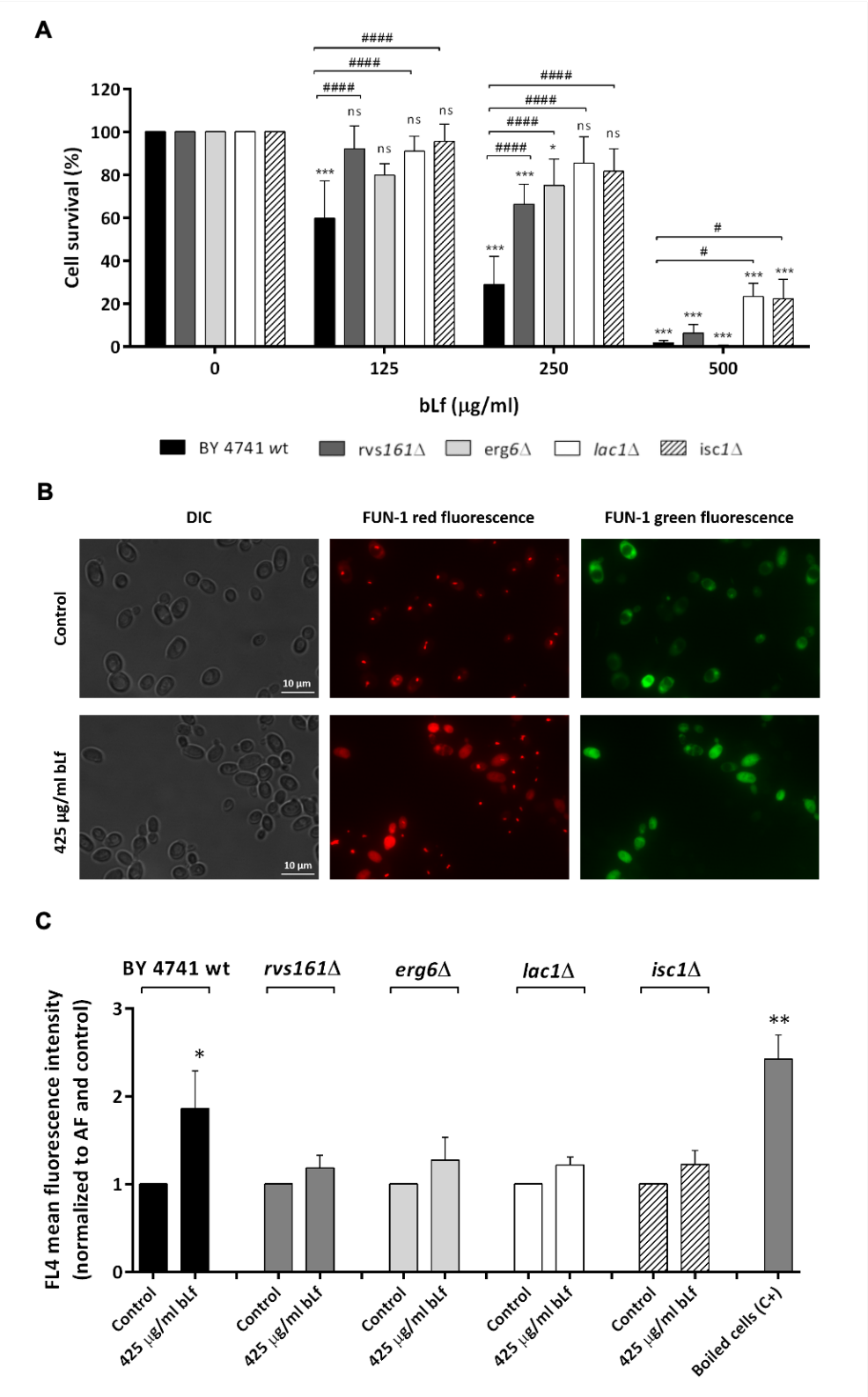

Figure 3 | Effect of bLf on cell survival and metabolic activity of wild type and *rvs161*Δ, *erg6*Δ, *lac1*Δ and *isc1*Δ mutant strains. (A) Cell survival assays of *S. cerevisiae* wild type BY4741 and indicated mutant strains after 90 min of incubation with 0-500 µg/ml bLf in 10 mM Tris-HCl buffer pH 7.4, at 30˚C, evaluated by colony forming unit counting. Values are mean ± standard deviation normalized to time zero of incubation and considering the control without bLf as 100% cell survival. **(B)** Fluorescence microscopy images showing FUN-1 staining of BY4741 wild type cells non-treated (control) or treated with 425 µg/ml bLf. **(C)** Flow cytometry analysis of FUN-1 staining of the same yeast strains treated as in A without or with 425 µg/ml bLf. 5 min-boiled cells were used as a control of dead cells (C+). Values represent mean ± standard deviation of red (FL4) fluorescence intensity normalized to autofluorescence of each sample and control of each strain. ns, non-significant; *, **, *** P<0.05, 0.01, 0.001, respectively, in comparison with the control of each strain; #, #### P<0.05, 0.0001, respectively, in comparison with the wild type strain.

We further demonstrated that the metabolic activity of the wild type strain is affected by the bLf treatment using FUN-1 staining (Fig. 3B, C). FUN-1 is a membrane-permeant dye that is first detected as diffuse green fluorescence in the cytosol, and then accumulates in the vacuole forming red cylindrical intravacuolar structures (CIVS), visualised as red spots in Fig. 3B, only in metabolically active yeast cells (Eggleston & Marshall 2007). Cells with metabolic alterations (such as heat-killed cells) are not able to process the dye at the vacuole and exhibit a bright diffuse fluorescence detected by an increase in the red fluorescence intensity in comparison with the cells exhibiting CIVS (Millard et al. 1997; Prudêncio et al. 1998; Pina-Vaz et al. 2001) (Fig. 3B). Hence, in the wild type strain, the red-emitting CIVS visualized in control cells indicate a high metabolic activity, whereas bright diffuse red and green-emitting fluorescence cells in bLf-treated sample correspond to metabolic inactive cells (Fig. 3B). We also analysed FUN-1 staining by flow cytometry where an almost 2-fold increase in the red mean fluorescence intensity was observed for the wild type strain, while for the mutants, no differences between treated and untreated cells were observed (Fig. 3C).

3. bLf does not alter localization of sterol-rich lipid rafts in *rvs161*Δ, *erg6*Δ, *lac1*Δ and *isc1*Δ mutants

As the cytotoxicity of bLf in the wild type strain was associated with intracellular accumulation of sterol-rich lipid rafts, the mutants under study were stained with filipin in the presence and absence of bLf. Results showed that bLf only affected ergosterol distribution in the wild type strain, having no effect on the mutants, which is in agreement with their higher survival rate upon treatment with bLf (Fig. 4A, B).

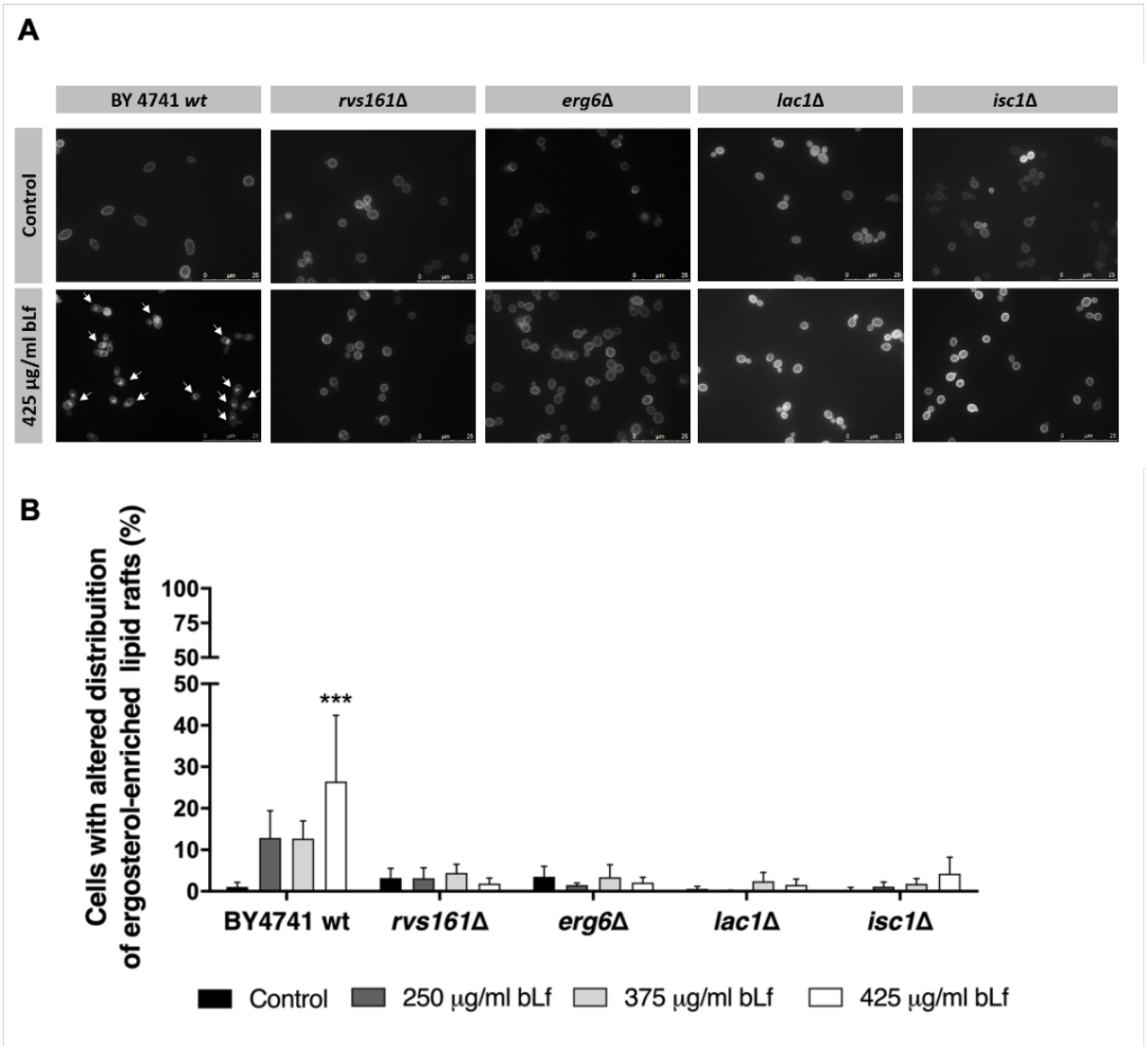

Figure 4 | Effect of bLf on the localization of sterol-rich lipid rafts of wild type and *rvs161*Δ, *erg6*Δ, *lac1*Δ and *isc1*Δ mutant strains. Cells were incubated in the absence or presence of increasing concentrations of bLf (250-425 µg/ml) for 90 min at 30˚C in Tris-HCl 10 mM pH 7.4 buffer. **(A)** For lipid rafts visualization, cells were stained in the dark with 0.1 mg/ml filipin immediately before visualization under the microscope. Representative fluorescence microscopy images of each condition are shown. Although *erg6*Δ cells do not synthetize ergosterol, they are still labelled with filipin as previously reported (Grossmann et al. 2008), because it also binds sterol intermediates. **(B)** Quantification of the percentage of cells with altered lipid rafts distribution. At least 300 cells per condition of three independent experiments were counted. *** P<0.001 in comparison with the control of each strain.

4. Inhibition of Pma1-proton pumping and hydrolytic activities by bLf is prevented in *rvs161*Δ, *erg6*Δ, *lac1*Δ and *isc1*Δ mutants

We next sought to test the hypothesis that the higher resistance of the mutants is due to the lack of sensitivity of their Pma1p to bLf inhibition. As shown in figure 5A, the Pma1p of

wild type cells was inhibited by bLf in a time- and concentration-dependent manner, much like it was previously observed in the pathogenic yeast *C. albicans* (Andrés et al. 2016). Diethylstilbestrol (DES) was used as a positive control of Pma1p inhibition (Andrés et al. 2016). When wild type cells were incubated with fluorescein-5-isothiocyanate (FITC)-labelled bLf, a punctuated pattern was observed at the plasma membrane (Fig. 5B), suggesting that Lf binds to Pma1p, as further confirmed by immunoprecipitation (Fig. 5F) and previously observed in *C. albicans* (Andrés et al. 2016). Contrarily to the result obtained in the wild type cells, bLf failed to inhibit Pma1p proton pumping activity of the mutant strains *rvs161*Δ, *erg6*Δ, *lac1*Δ and *isc1*Δ, as indicated by the unperturbed extracellular acidification rates (Fig. 5C). Accordingly, when the hydrolytic activity of Pma1p was measured, the inhibitory effect of bLf over Pi release was much less pronounced in plasma membrane fractions isolated from the mutant strains than from wild type cells. In agreement, incubation of intact cells with bLf led to an increase in intracellular accumulation of ATP in the wild type strain but not in the mutant strains (Fig. 5E). Immunoprecipitation experiments revealed that, although Pma1p activity is not affected by bLf in the mutant strains, bLf is still able to bind the proton pump (Fig. 5F, G) in these strains.

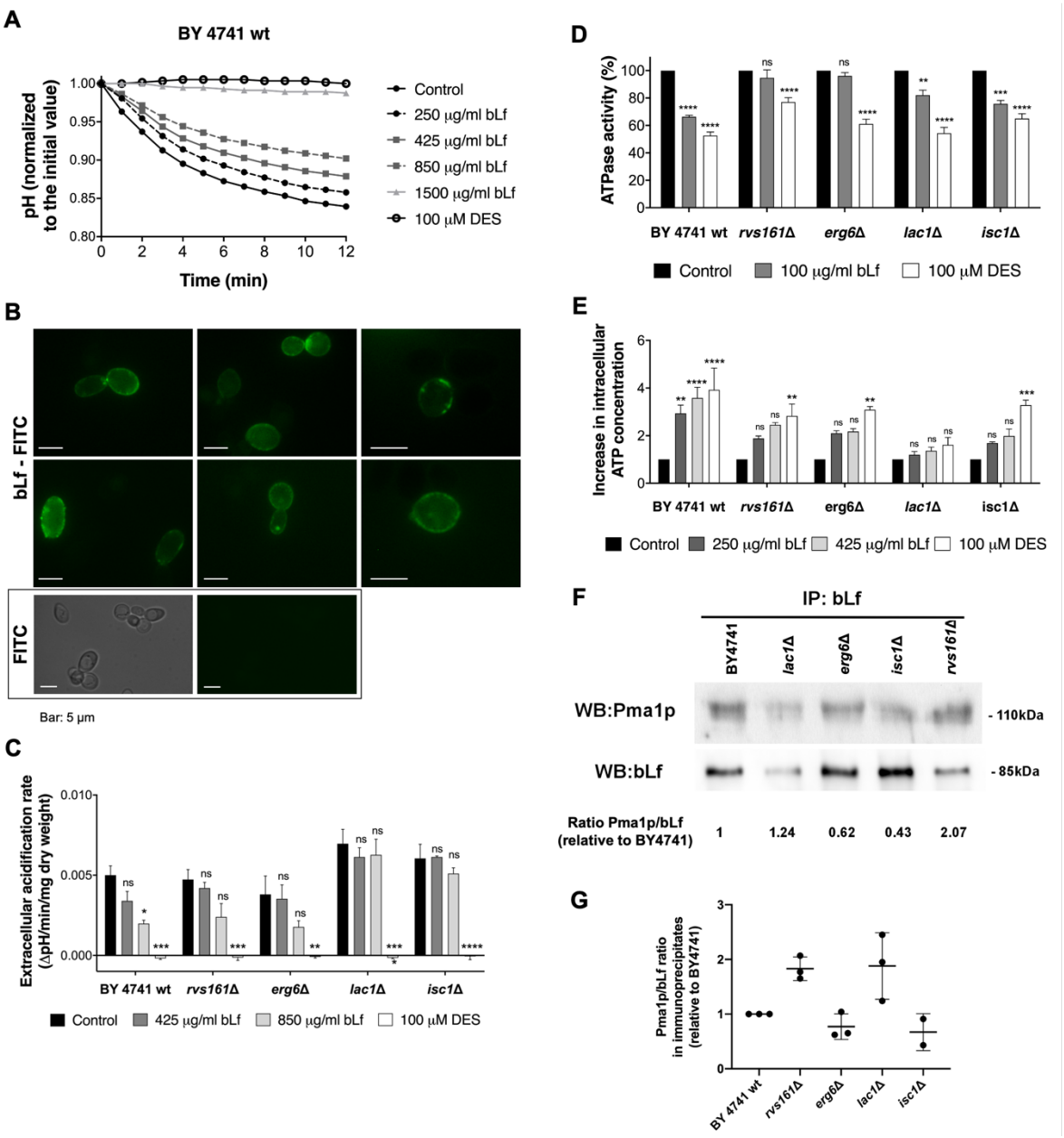

Figure 5 | Effect of bLf on Pma1p activity of wild type and *rvs161*Δ, *erg6*Δ, *lac1*Δ and *isc1*Δ mutant strains. **(A)** Pma1p proton pumping activity was assessed by measuring glucose-induced external pH variation using a pH electrode. BY4741 wild type cells were incubated for 90 min in 10 mM Tris-HCl buffer pH 7.4 with 0-1500 µg/ml bLf or 100 µM DES. After pH stabilization, 2.5 mM glucose was added to induce proton extrusion by Pma1p and pH values were monitored every minute up to 12 min. Data are pH values normalized to the value at timepoint zero min. **(B)** Localization of bLf-FITC (fluorescein-5-isothiocyanate) (500 µg/ml) in the wild type cells after 75 min of incubation in the same conditions as in A. A control with only FITC was performed under the same conditions to ensure a specific labelling. Bar: 5 µm **(C)** Same as in A but with wild type and indicated mutant strains treated with 0, 425 or 850 µg/ml bLf or 100 µM DES. Values are expressed as the pH variation per min per mg of dry weight of four independent experiments. **(D)** ATPase activity of isolated plasma membranes of the indicated strains expressed as percentage in comparison with the control of each strain of three independent experiments. Membranes were treated for 15 min without or with 100 µg/ml bLf or 100 µM DES in

10 mM Tris-HCl pH 7.4 buffer containing 0.2 mM $(NH_4)_2MoO_4$, 5 mM NaN_3, and 50 mM KNO_3 to inhibit acid phosphatase, mitochondrial and vacuolar ATPases, respectively. **(E)** Measurement of intracellular ATP levels of cells incubated for 90 min with 0, 250 or 425 μg/ml bLf or 100 μM DES. Values represent the increase in ATP level expressed in folds in comparison with the control of each strain of three independent experiments. ns, non-significant; *, **, ***, ****, P<0.05, 0.01, 0.001, 0.0001, respectively, in comparison with the control of each strain. **(F)** Representative western blot of the immunoprecipitation between bLf and Pma1p in bLf-treated wild type and mutant strains. **(G)** Quantification of Pma1p/bLf ratio in relation to the wild type strain in the immunoprecipitates of three independent experiments.

To determine whether these phenotypes could be related to intrinsic differences in Pma1p activity/localization in the mutant strains under study, all strains were transformed with a pRS316 Pma1-GFP plasmid and stained with filipin to visualize lipid rafts. Fluorescence microscopy showed that Pma1p co-localizes at the plasma membrane with lipid rafts in all strains (Fig. 6A). Additionally, immunodetection of Pma1p by western blot demonstrated that the expression levels of this proton pump are similar in all strains (Fig. 6B, C). Moreover, Pma1p activity of the mutant strains, expressed by the extracellular acidification rate, is similar to the wild type thus demonstrating that Pma1p is functional in the mutant strains (Fig. 6D). Altogether, our data indicate that despite similar intrinsic Pma1p localization, expression, activity and bLf binding to Pma1p in the mutant strains in comparison with the parental strain, lack of inhibition of both Pma1p proton pumping and hydrolytic activities underlies the higher resistance of the mutants to the bLf cytotoxic effect.

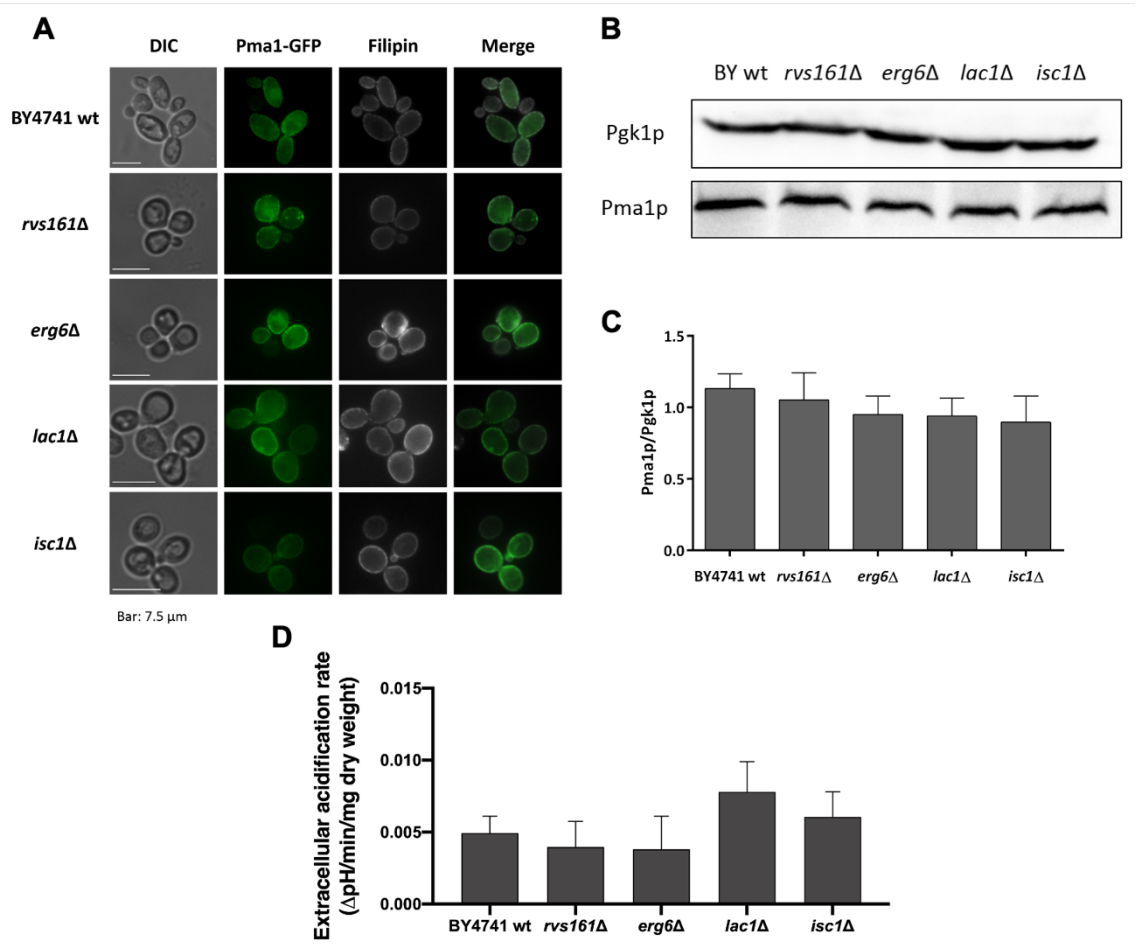

Figure 6 | Pma1p localization, expression levels and proton pumping activity of wild type and *rvs161*Δ, *erg6*Δ, *lac1*Δ and *isc1*Δ mutant strains. (A) Cells transformed with pRS316 Pma1-GFP plasmid were stained with 0.1 mg/ml filipin and visualized under a fluorescence microscope with green (Pma1-GFP) and blue (filipin) channels. DIC images are also shown and images are representative of each condition. Bar: 7.5 µm. **(B)** Representative western blot image of endogenous Pma1p expression levels in each strain. Pgk1p was used as loading control. **(C)** Quantification of Pma1p expression levels normalized to Pgk1p levels. Values represent the mean of three independent experiments. (D) Pma1p proton pumping activity was assessed by measuring glucose-induced external pH variation using a pH electrode. After pH stabilization, 2.5 mM glucose was added to induce proton extrusion by Pma1p and pH values were monitored every minute up to 12 min. Values are expressed as the pH variation per min per mg of dry weight of four independent experiments. Values represent the mean of four independent experiments.

5. bLf-induced vacuolar pH perturbations are prevented in *rvs161Δ, erg6Δ, lac1Δ and isc1Δ*

Since we previously reported that bLf targets and inhibits plasmalemmal V-ATPase in highly metastatic cancer cells (Pereira et al. 2016; Guedes et al. 2018), we then monitored the effect of bLf on V-ATPase proton pumping activity in purified vacuolar fractions isolated

from the wild type yeast strain. Results depicted in Fig. 7A demonstrate for the first time that bLf inhibited the yeast V-ATPase proton pumping activity in a concentration-dependent manner, much like it was previously reported in cancer cells.

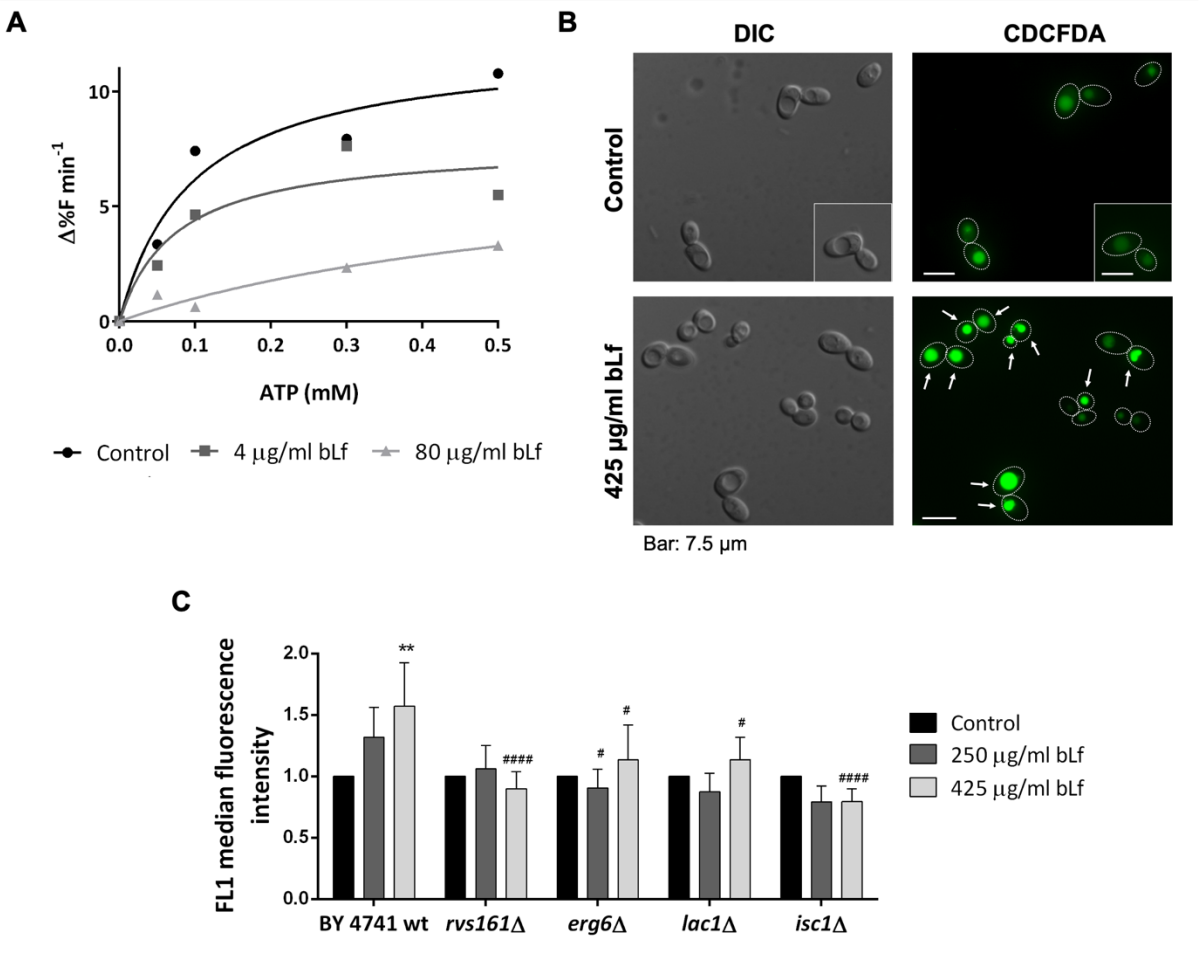

Figure 7 | Effect of bLf on V-ATPase and vacuolar pH. (A) Kinetics of ATP-dependent V-ATPase proton pumping activity of vacuoles isolated from the wild type BY 4741 strain before (control) and after addition of 4 and 80 µg/ml bLf. The continuous lines are derived by fitting the data points to a Michäelis–Menten kinetics. Vacuolar suspensions were previously stained with the pH-sensitive probe ACMA and analysed by spectrofluorimetry after addition of increasing concentrations of ATP. **(B)** Representative fluorescence microscopy images of BY4741 wild type cells incubated in the absence (control) or presence of 425 µg/ml bLf for 90 min at 30˚C in Tris-HCl 10 mM buffer pH 7.4 and then stained with CDCFDA. White arrows indicate cells with increased vacuolar fluorescence. Bar: 7.5 µm. **(C)** Quantification of the green median fluorescence intensity of BY4741 wild type and *rvs161*Δ, *erg6*Δ, *lac1*Δ and *isc1*Δ mutant strains treated in the same conditions without and with 250 or 425 µg/ml bLf. Values are median of three independent experiments normalized to T0 and control of each strain. ** P<0.01 in comparison with the control of each strain; #, #### P<0.05; 0.0001, respectively, in comparison with the same condition in the wild type strain.

When wild type yeast cells were labelled with the pH-sensitive probe 5-(and-6)-carboxy-2,7-dichlorofluorescein diacetate (Carboxy-DCFDA), a higher fluorescence signal was observed in bLf-treated than in untreated cells by both fluorescence microscopy (Fig. 7B, white arrows) and flow cytometry (Fig. 7C). This fluorescent probe is cleaved by intracellular esterases, and the unsterified pH-sensitive form (CDCF) accumulates in the yeast vacuole exhibiting higher fluorescence with higher pH values (Roberts et al. 1991; Teixeira et al. 2009). The vacuolar alkalinization in wild type cells suggests an inhibition of V-ATPase activity by bLf that does not occur in the mutant strains (Fig. 7C), which may contribute to their higher survival rate upon bLf treatment.

6. Disruption of Pma1p-lipid rafts association induced by Pma1p point mutations or *AST1* deletion renders yeast cells resistant to bLf

To get further insights on the role of Pma1p localization at the lipid rafts for bLf-induced cytotoxicity, we next explored the effect of bLf on a strain harbouring Pma1p point mutations that alter its localization and association with lipid rafts. Pma1-10 (XGY32 strain) harbours the A165G and V197I mutations, both at the first cytoplasmic loop between transmembrane segments 2 and 3 of Pma1p. In this mutant strain, at the restrictive temperature of 37ºC, newly synthesized Pma1-10 fails to associate with the plasma membrane lipid rafts (Triton-insoluble fraction), goes to the vacuole and suffers vacuolar degradation (Gong & Chang 2001). Cell survival assays of the L3852 wild type and Pma1-10 mutant strains treated with 75 ug/ml bLf at 30˚C and 37˚C showed that the Pma1-10 expressing cells are more resistant to bLf than the wild type strain, especially at 37˚C (Fig. 8A). In this experiment, a lower bLf concentration was used because the wild type strain is more sensitive to bLf than the BY4741 strain.

Ast1p is a Pma1p-binding protein known to be involved in the delivery of Pma1p to the cell surface and its association with lipid rafts. When multicopy *AST1* is expressed in mutated Pma1p cells, Pma1p is rerouted to the cell surface and associates with lipid rafts (Chang & Fink 1995; Bagnat et al. 2001). The deletion of *AST1* gene renders cells more resistant to bLf, suggesting that its function in promoting the association of Pma1p with lipid rafts is critical for bLf cytotoxicity. Accordingly, when multicopy *AST1* is expressed in this background, cells become sensitive to bLf again, thus demonstrating that the resistance is indeed related with *AST1* deletion, and not with other possible pleiotropic effects (Fig. 8B). When Pma1-GFP was expressed in *ast1*Δ cells, about 30% of cells exhibited bright intracellular spots of Pma1-GFP (Fig. 8C, D) suggesting that Pma1p localization is affected in this strain. We then

addressed lipid rafts localization in the *ast1*Δ strain and found that, although both sterol-rich lipid rafts and Pma1p are located at the plasma membrane in some cells (in agreement with the previous results), there are also cells in which both are affected, exhibiting an abnormal intracellular localization, which is consistent with the role of Ast1p in Pma1p-lipid rafts association (Fig. 8E).

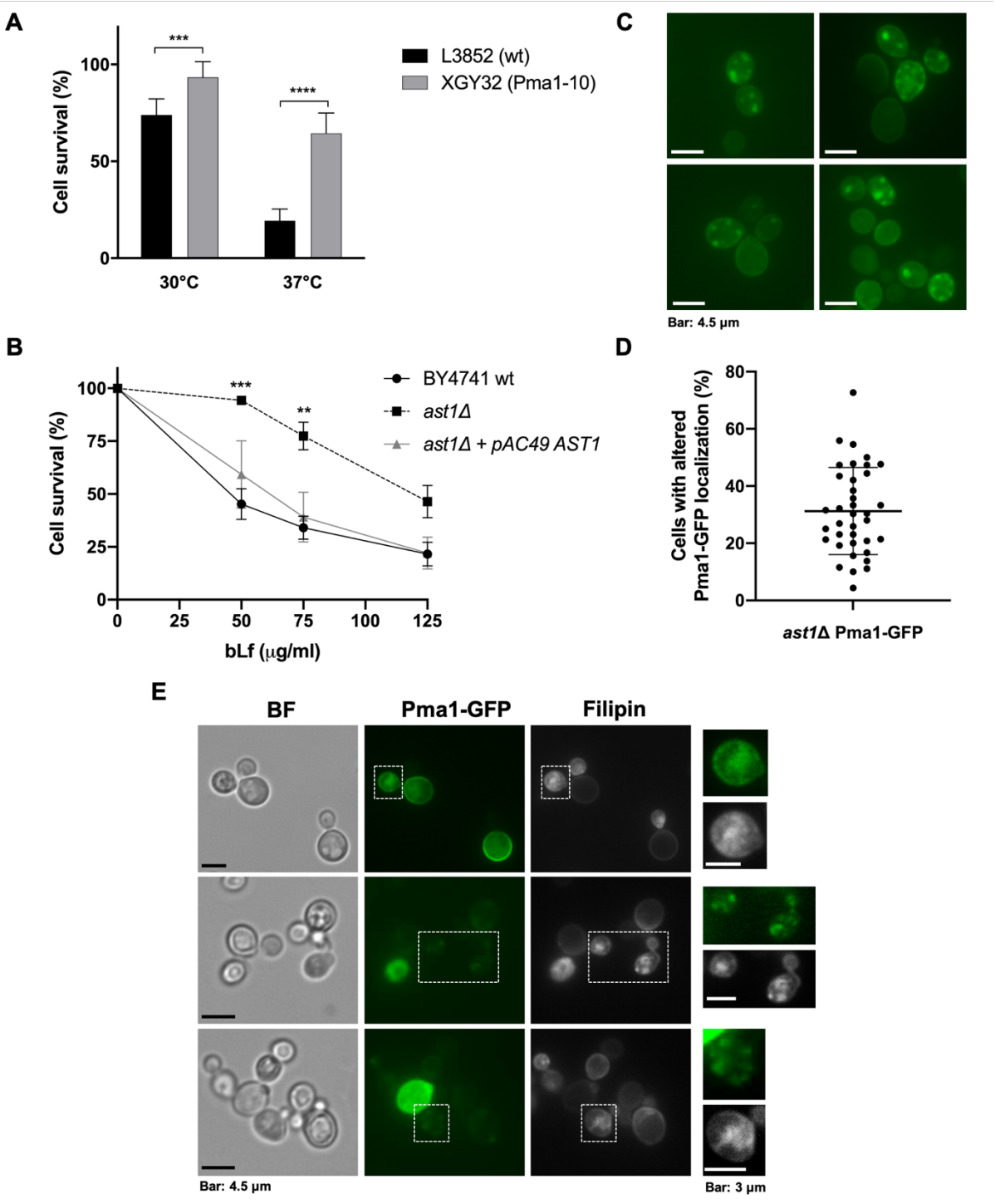

Figure 8 | Effect of bLf on cell survival of strains with defective association of Pma1p with lipid rafts or lacking Ast1p. (A) L3852 wild type and Pma1-10 (XGY32) expressing cells were pre-grown at 30˚C until OD_{640nm}=0.7 and then shifted or not to 37˚C in the absence or presence of 75 µg/ml bLf in 10 mM Tris HCl pH 7.4 buffer for 90 min. Values are percentage of cell survival assuming the control without bLf as 100% cell survival. **(B)** BY4741 wild type, *ast1*Δ and *ast1*Δ+pAC49 AST1 strains treated with 50 to 125 µg/ml bLf in 10 mM Tris HCl buffer pH 7.4 for 90 min at 30 ˚C. Values are percentages normalized to the control without bLf of each strain (considered as 100% cell survival). **, *** P<0.01, 0.001, respectively, in comparison with the wild type strain in the same condition. **(C)** *ast1*Δ cells expressing pRS316 Pma1-GFP were grown until exponential phase and observed under the fluorescence microscope for observation of Pma1p localization. **(D)** Percentage of *ast1*Δ cells with altered Pma1p localization. The individual percentual values of each observed field as well as the mean and standard deviation are presented. More than 800 cells were counted. **(E)** *ast1*Δ cells expressing pRS316 Pma1-GFP were grown in the same conditions as in C and D. For lipid rafts visualization, cells were stained in the dark with 0.1 mg/ml filipin immediately before visualization under the microscope. Right images are the zoom in with higher exposure of the indicated sections of the whole images. Bars: 4.5 µm or 3 µm, as indicated in the figure.

DISCUSSION

It has been reported that the milk-derived protein Lf displays antifungal activity against different yeast species (Fernandes et al. 2020), including *C. albicans* (Andrés et al. 2008) and *S. cerevisiae* (Acosta-Zaldívar et al. 2016), as well as against different fungi isolated from plants and soils including *Aspergillus niger* and *Rhizoctonia solani* (Lahoz et al. 2008). Given its potential to become a wide-spectrum antifungal, herein we sought to deepen our understanding of the mechanisms underlying Lf cytotoxic activity using *S. cerevisiae* as a model. As we previously showed in *C. albicans* (Andrés et al. 2016; Andrés et al. 2019), we found that bLf binds to Pma1p and inhibits its proton pumping and hydrolytic activities associated with enhancement of the intracellular ATP levels. Since lipid rafts are important for cell surface sorting, stability and oligomerization of Pma1p (Bagnat et al. 2001), we investigated the effect of bLf in these sterol- and sphingolipid-rich membrane microdomains. Our data revealed a novel mode of action of bLf against yeast by perturbing the localization of sterol-rich lipid rafts. Indeed, bLf-treated cells exhibited intracellular accumulation of sterol-rich lipid rafts in contrast with the typical punctuated pattern at the plasma membrane of control cells. This mechanism of action is shared with edelfosine, a compound that, like lactoferrin, exhibits anticancer activity (Zaremberg et al. 2005; Pereira et al. 2016; Guedes et al. 2018) and a marked activity against yeast (Zaremberg et al. 2005; Acosta-Zaldívar et al. 2016). Indeed, it was found that edelfosine displaces sterols from the plasma membrane and

induces loss of Pma1p from lipid rafts (Zaremberg et al. 2005). However, it is noteworthy that the bLf effect on lipid rafts differs from MβCD, which is known to disrupt lipid rafts by depleting ergosterol from the plasma membrane (Siafakas et al. 2006). Indeed, while both compounds led to intracellular accumulation of sterol-rich lipid rafts, in contrast to MβCD, bLf-treated cells still preserved these structures at the plasma membrane, as visualized by the intracellular and plasma membrane filipin staining. This suggests that bLf impairs the sorting of newly synthetized lipid rafts to the cell surface, rather than sequestering them from the plasma membrane.

In order to gain insights on the importance of lipid rafts integrity for bLf antifungal activity, a comprehensive characterization of the phenotype of mutant strains lacking the lipid rafts-associated proteins Rvs161p, Erg6p, Lac1p or Isc1p was performed. Ergosterol plays crucial roles in bulk membrane functions and in lipid rafts formation as it is essential for membrane fluidity, permeability and rigidity and for the protein sorting along the secretory pathway (Umebayashi & Nakano 2003; Abe & Hiraki 2009). In *erg6*Δ mutants, the accumulated ergosterol precursors do not allow a tight packing of the lipid bilayer, specifically the lipid acyl chains, and are suggested to create voids in the plasma membrane (Abe & Hiraki 2009). Accumulation of ergosterol intermediates can also alter lipid rafts structures, promote missorting of different plasma membrane proteins (Daicho et al. 2009) and modify membrane permeability and fluidity (Gaber et al. 1989). Sphingolipids are a multifunctional class of lipids critical for lipid rafts formation and for many other functions including the transport of glycosylphosphatidylinositol (GPI)-anchored proteins out of the endoplasmic reticulum, protein sorting and signalling (Martinez-Montanes et al. 2016). In yeast, ceramides can be produced either *de novo* through Lag1p/Lac1p/Lip1p, or from complex sphingolipids hydrolysis through Isc1p (Cowart & Obeid 2007). *LAC1* and *LAG1* are highly homologous and have a similar function; along with a small accessory subunit Lip1p, Lac1p and Lag1p are demonstrated constituents of the ceramide synthase complex (Schorling et al. 2001). Deletion of both genes influences the levels of ceramides and long chain bases (Guillas et al. 2001; Schorling et al. 2001). Yeast cells lacking Lac1p have an abnormal low amount of GPI-anchored proteins and have problems introducing the ceramide moiety into GPI anchors, which are very important for the association of different proteins to lipid rafts (Guillas et al. 2001; Kinoshita & Fujita 2016). The *ISC1* gene encodes the mitochondrial inositol phosphosphingolipid phospholipase C that is involved in the synthesis of ceramide by hydrolysis of the head groups of complex sphingolipids (Cowart & Obeid 2007). Thus, *isc1*Δ cells contain higher amount of complex sphingolipids (Sawai et al. 2000), decreased levels of

mitochondrial ceramide and mitochondrial function defects (Kitagaki et al. 2007). Another mutant that was studied herein lacks Rvs161 protein, a lipid rafts component involved in cytoskeleton organization, cell polarity, endocytosis and in vesicle trafficking (Breton et al. 2001; Balguerie et al. 2002). Its association with the lipid rafts is thought to be mediated by a putative raft-bound protein as it has no GPI signal anchor or transmembrane domain (Balguerie et al. 2002). We found that cells lacking Rvs161p, Lac1p, Isc1p and Erg6p are more resistant to bLf-induced cell death than the wild type strain and exhibit a lower inhibition of the extracellular acidification rate and hydrolytic activity and no enhancement of the intracellular ATP level. These results suggest that normal levels of ergosterol, sphingolipids and lipid rafts-associated proteins determine the bLf killing activity against yeast. We hypothesized that changes in Pma1p localization, expression and activity in the mutant strains could explain the reduced cytotoxic effects of bLf. However, this hypothesis was discarded as Pma1p localization and levels of expression and activity of the mutants were identical to those of the wild type strain. The results regarding the *erg6*Δ mutant are in agreement with previous works showing that Pma1p localization at the plasma membrane was intact in different *erg* mutants (Gaigg et al. 2005; Estrada et al. 2015), and that the extracellular medium acidification kinetics in the *erg24*Δ mutant was identical to the wild type strain (Zhang et al. 2010). Moreover, it was shown that deletion of *ISC1* in *Cryptococcus neoformans* did not affect the synthesis and transport of Pma1p (Farnoud et al. 2014). Unexpectedly, the inhibition of Pma1p activity by bLf was not associated with lack of Pma1p-bLf binding since this was not abrogated in the mutant strains. In addition, bLf was unable to perturb the sterol-rich lipid rafts distribution in the mutant strains, indicating that this bLf-induced alteration is also dependent on the normal composition of lipid rafts. Altogether this suggests that the perturbation of lipid rafts is intimately related with Pma1p inhibition, and both effects seem to depend on each other.

Evidence supporting the hypothesis that bLf requires the integrity of Pma1p-lipid rafts association to inhibit Pma1p and induce yeast cell dead, was provided by the experiments with the strain harbouring Pma1p point mutations and with the *ast1*Δ strain. Pma1-10 mutation renders a defective association of Pma1p with the lipid rafts at 37°C (Gong & Chang 2001), temperature at which the strain became much more resistant to bLf than the wild type strain. At a permissive temperature, where Pma1-10 is associated with the lipid rafts, the sensitivity to bLf was similar to the wild type cells. In addition, deletion of the *AST1* gene that encodes a protein involved in Pma1p association with the lipid rafts (Bagnat et al. 2001), rendered yeast cells resistant to bLf, and its overexpression in the deletion background

restored the sensitivity to bLf. The Pma1p and lipid rafts distribution are affected in the *ast1*Δ strain, supporting that alteration of Pma1p-lipid rafts association underlies the bLf-resistance phenotype of this strain.

Besides being involved in the association of Pma1p with lipid rafts, Ast1p was also demonstrated to induce Pma1p oligomerization, which is an early event during the surface delivery of Pma1p (Bagnat et al. 2001). Pma1p forms large oligomeric complexes of about 1 MDa (Lee et al. 2002) and this process seems to be affected by alterations in sphingolipids synthesis. Indeed, deletion of *ISC1* in *C. neoformans* perturbed Pma1p oligomerization, which was restored after supplementation with phytoceramide (Farnoud et al. 2014). Depletion of sphingolipids either by using the *lcb1-100* strain, which is unable to synthetize sphingolipids, or myriocin, an inhibitor of serine palmitoyltransferase activity, inhibits the oligomerization of newly synthetized Pma1p. Addition of the ceramide precursor phytosphingosine restored Pma1p oligomerization, reinforcing the importance of sphingolipid levels for Pma1p oligomerization (Lee et al. 2002). Accordingly, the requirement of sphingolipids for Pma1p oligomerization at the ER, plasma membrane targeting, stability and acquisition of detergent resistance of Pma1p was reported by different authors (Wang & Chang 2002; Gaigg et al. 2005). In agreement with these data, herein we found that exogenous addition of C2-ceramide reverts the resistance phenotype of the *lac1*Δ mutant strain to bLf, likely by counteracting defects in Pma1p oligomerization as a result of sphingolipids composition reestablishment (Fig. S1). Hence, the most likely explanation for the mutant resistance phenotypes is that alterations in the lipidic content of cells, namely unbalanced ceramide/complex sphingolipids ratio, accumulation of ergosterol precursors, or the abnormal production of GPI anchors modifies the composition of plasma membrane lipid rafts, affecting Pma1p conformation and oligomerization, and consequently its inhibition by bLf. Accordingly, it has been suggested that perturbation of the lipid rafts functional organization creates a different biophysical environment that may change the conformation of raft-localized proteins, including Pma1p (Pan et al. 2018).

Another novelty of the present study is the inhibition of the V-ATPase by bLf. Indeed, we showed that bLf inhibits the activity of this proton pump in purified vacuoles from the wild type strain and also increases the vacuolar pH in whole cells. As for the strains with altered lipid raft composition, the vacuolar pH was not affected most likely due to the inability of bLf to inhibit Pma1p and cause intracellular acidification. Nonetheless we cannot discard the hypothesis of an incapacity of bLf to inhibit the V-ATPase as a consequence of the alteration of vacuolar membrane lipid composition. These results are in accordance with

our previous data showing that bLf inhibits the activity of the V-ATPase that is targeted to the plasma membrane of highly metastatic cancer cells as well as the activity of purified rat liver lysosomes V-ATPase (Pereira et al. 2016) and increases lysosomal pH of highly metastatic cancer cells (Guedes et al. 2018).

In summary, our data demonstrate that the mode of action underlying bLf antifungal activity lies on the perturbation of lipid rafts organization and inhibition of Pma1p activity, and likely of V-ATPase activity, as suggested by our data with isolated vacuoles and whole cells (Fig. 9). Moreover, the normal composition of the plasma membrane lipid rafts, Pma1p oligomerization status as well as the integrity of Ast1p-mediated lipid rafts-Pma1p association seems to be crucial for the interaction of bLf with Pma1p, and for its killing activity against *S. cerevisiae*. We propose that this novel bLf lipid rafts disrupting activity may be explored towards antifungal therapy alone or in combination with classical antifungals.

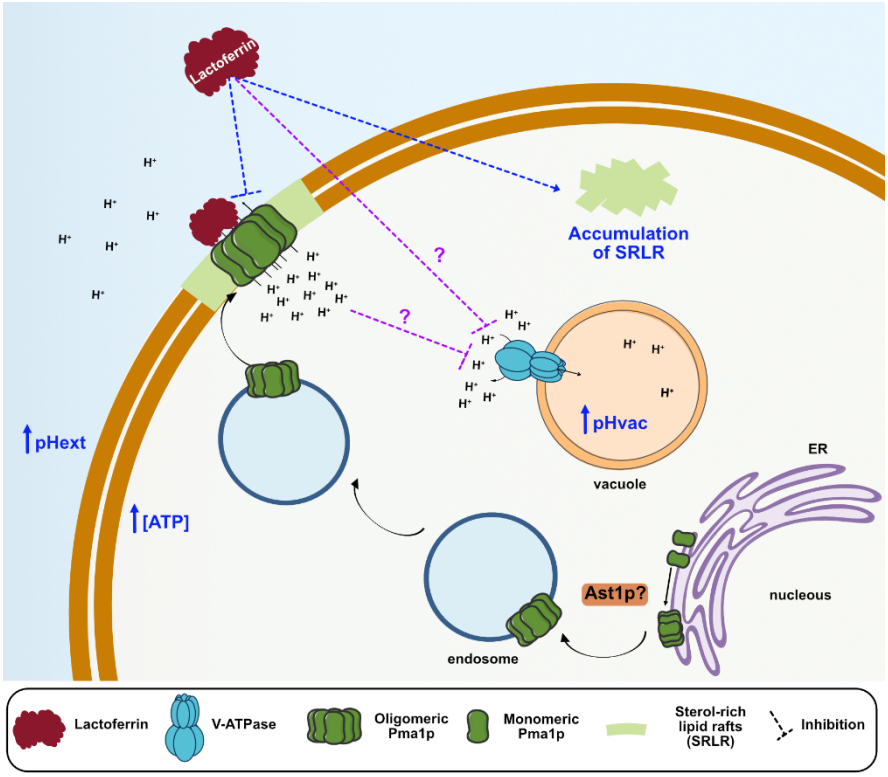

Figure 9 | Model representation of the mode of action underlying bovine lactoferrin antifungal activity. Exposure of yeast cells to bLf leads to inhibition of Pma1p, associated with an inhibition of the extracellular acidification rate and consequent enhancement of intracellular proton accumulation and ATP concentration. In addition, bLf could directly inhibit V-ATPase as observed with purified vacuoles or indirectly through intracellular acidification (Dechant et al. 2010), leading to vacuolar alkalinisation. Moreover, bLf binds to Pma1p and induces intracellular accumulation of sterol-rich lipid rafts (SRLR). Our data together with evidence from the literature led to the hypothesis that Pma1p oligomerization may be important for bLf-mediated Pma1p

inhibition, although further work is required. The Pma1p-interacting protein Ast1p may also play a role in this process. Oligomerization of Pma1p is suggested to occur at the ER (Toulmay & Schneiter 2007) and the involvement of Ast1p in the process seems to be an early event during plasma membrane delivery (Bagnat et al. 2001). pHext (extracelular pH), pHvac (vacuolar pH), ER (endoplasmic reticulum).

MATERIALS AND METHODS

Strains and plasmids

All *S. cerevisiae* strains and plasmids used in this study are listed in Table 1. BY4741 and L3852 were used as wild type strains. BY4741, *erg6*Δ, *rvs161*Δ, *lac1*Δ, *isc1*Δ and *ast1*Δ strains were transformed with the pRS316 Pma1-GFP using the LiAc/SS Carrier DNA/PEG method (Gietz & Woods 2006). The *ast1*Δ strain was transformed with the high copy pAC49 AST1 plasmid using the same method. The XGY32 strain harbours the *pma1-10* mutations and it was produced by pop-in pop-out gene replacement of the *PMA1* gene (Gong & Chang 2001).

Table 1: List of *S. cerevisiae* strains and plasmids used throughout this study.

Strain	**Genotype**	**Reference/ Source**
BY4741	MATa his3Δ1 leu2Δ0 met15Δ0 ura3Δ0	Euroscarf
*erg6*Δ	MATa his3Δ1 leu2Δ0 met15Δ0 ura3Δ0 *erg6*Δ::KanMX4	Euroscarf
*rvs161*Δ	MATa his3Δ1 leu2Δ0 met15Δ0 ura3Δ0 *rvs161*Δ::KanMX4	Euroscarf
*lac1*Δ	MATa his3Δ1 leu2Δ0 met15Δ0 ura3Δ0 *lac1*Δ::KanMX4	Euroscarf
*isc1*Δ	MATa his3Δ1 leu2Δ0 met15Δ0 ura3Δ0 *isc1*Δ::KanMX4	Euroscarf
*ast1*Δ	MATa his3Δ1 leu2Δ0 met15Δ0 ura3Δ0 *ast1*Δ::KanMX4	Euroscarf
BY4741	BY4741 harboring pRS316 *PMA1*-GFP	This study
*erg6*Δ *PMA1*-GFP	*erg6*Δ harboring pRS316 *PMA1*-GFP	This study
*rvs161*Δ *PMA1*-GFP	*rvs161*Δ harboring pRS316 *PMA1*-GFP	This study
*lac1*Δ *PMA1*-GFP	*lac1*Δ harboring pRS316 *PMA1*-GFP	This study
*isc1*Δ *PMA1*-GFP	*isc1*Δ harboring pRS316 *PMA1*-GFP	This study

*ast1*Δ *PMA1*-GFP	*ast1*Δ harboring pRS316 *PMA1*-GFP	This study
*ast1*Δ *AST1*	*ast1*Δ harboring pAC49-*AST1*	This study
L3852	MATa his3Δ200 lys2Δ201 leu2-3,112 ura3-52 ade2	(Chang & Fink 1995)
XGY32	MATα his3Δ200 lys2Δ201 leu2-3,112 ura3-52 ade2 *pma1-10*	(Gong & Chang 2001)
Plasmid	**Description**	**Reference**
pRS316 Pma1-GFP	URA3, *PMA1* gene fused with the yeast *GFP3* gene	(Balguerie et al. 2002)
pAC49-*AST1*	*AST1* URA3 2μ	(Chang & Fink 1995)

Growth conditions

All strains were grown in YEPD (yeast extract-peptone-dextrose) medium [1% (w/v) yeast extract, 2% (w/v) peptone, 2% (w/v) glucose], with the exception of the strains expressing plasmids that were grown in Synthetic Complete Glucose medium [SC Glu pH 5.5; 2% (w/v) glucose; 0.67% (w/v) yeast nitrogen base without amino acids and ammonium sulphate; 0.5% (w/v) ammonium sulphate; 0.1% potassium phosphate, 0.2% (w/v) drop-out mixture lacking histidine, leucine, tryptophan and uracil; 0.01% (w/v) histidine, 0.02% (w/v) leucine and 0.01% (w/v) tryptophan]. The yeast strains were grown at 30˚C in an orbital shaker at 200 rpm, with a ratio of flask volume/medium of 5:1 until reaching the exponential phase (OD_{640} = 0.6-0.8).

Lactoferrin treatment and cell survival assays

After reaching the exponential phase, yeast cells were harvested, resuspended in 10 mM Tris-HCl buffer pH 7.4 (Acosta-Zaldívar et al. 2016) and incubated with 0-850 μg/ml bLf and/or with 20 μM C2-ceramide (N-Acetyl-D-sphingosine, Sigma-Alrich) or its solvent (absolute ethanol) for 90 min under the same conditions (and/or at 37˚C in the case of L3852 and XGY32 strains). bLf was obtained from DMV (Veghel, The Netherlands). The protein is ca. 80% pure, with 3.5% moisture, and 21% iron-saturated, according to the manufacturer. bLf was dissolved in sterile distilled water (dH_2O) to obtain the different concentrations used throughout this work.

Cell survival was evaluated by counting of colony forming units (c.f.u.). Briefly, four serial dilutions of the cultures were performed, and the 10^{-4} dilution was plated onto YEPD

containing 2% (w/v) agar and incubated for 48h at 30˚C. The percentage of cell survival was calculated from the number of c.f.u. of each condition in relation to time zero and the control without any treatment.

Filipin staining, Pma1-GFP localization and fluorescence microscopy

For visualization of sterol-rich lipid rafts, yeast cells were stained with filipin (Filipin III from *Streptomyces filipinensis*, Sigma), a naturally fluorescent antibiotic widely used to visualize sterols (Maxfield & Wüstner 2012). After treatment with or without bLf, cells were collected at an OD_{640} = 0.5 and concentrated 20× in sterile water. Immediately before visualization under the fluorescence microscope, cells were incubated for 1 min in the dark with 0.1 mg/ml filipin from a stock solution of 5 mg/ml (w/v) in methanol (Pacheco et al. 2013). Cells were then mounted on slides with the anti-fading agent Vectashield (Vector Laboratories) to overcome the instability of this dye, and then visualized in an epifluorescence microscope. As a positive control of lipid rafts disruption, cells were treated for 30 min at 30˚C in an orbital shaker at 200 rpm with 5 mg/ml methyl-β-cyclodextrin (MβCD) in 10 mM Tris-HCl buffer pH 7.4.

For determination of Pma1p localization, Pma1-GFP expressing cells without any treatment were grown until early-exponential phase, collected by centrifugation at 3000×*g* for 3 min, and resuspended in sterile water at an OD=10. Samples were observed under the fluorescence microscope immediately. The percentage of cells with altered Pma1p localization was calculated by counting the number of cells with normal and altered Pma1p localization in each observed field. More than 800 cells were counted.

The images were obtained in the fluorescence microscope (Leica DM 5000B, Leica Microsystems) with appropriate filter settings using a 100× oil-immersion objective with a Leica DCF350FX digital camera, and processed with LAS Leica Microsystems software.

Lactoferrin-FITC labelling

For labelling of bLf with fluorescein-5-isothiocyanate (FITC), 50 µg/ml of FITC (Sigma-Aldrich) were added to a solution of 18,13 mg/ml of bLf in 1M sodium bicarbonate buffer pH=9 and incubated for 2h in the dark with agitation. Afterwards, the unbound FITC was removed by several spin-separation cycles at 6000 ×*g* for 5 min using Amicon Ultra-0.5, Ultracel-30 Membrane (30 kDa cutoff), and finally buffer exchange to water was performed using the same approach. A control with only FITC was performed and added to cells. No fluorescence was detected using the same settings as those for bLf-FITC.

Assessment of metabolic activity by FUN-1 staining

Metabolic activity of yeast cells was evaluated by Fun-1 [(2-chloro-4-(2,3-dihydro-3-methyl-(benzo-1,3-thiazol-2-yl)-methylidene)-1-phenylquinolinium Iodide), Molecular Probes] staining. Fun-1 is a membrane-permeant dye that is transported to the vacuole and compacted into cylindrical intravacuolar structures (CIVS) only in metabolically active yeast cells (Millard et al. 1997). After incubation in the absence or presence of 250 or 475 µg/ml bLf, 1 mL of cells at OD_{640nm}=0.1 were harvested, resuspended in phosphate buffered saline (PBS) 1× (PBS 10×; 137 mM NaCl, 2.7 mM KCl, 10 mM Na_2HPO_4, 1.8 mM KH_2PO_4, pH 7) and stained with 4 µM FUN-1 for 30 min at 30˚C in the dark. 5 min-boiled wild type cells were used as a positive control for defective metabolic activity. Stained cell suspensions were then analysed in an epifluorescence microscope and in a flow cytometer. Flow cytometry data are presented as the mean FL4 fluorescence intensity in relation to the autofluorescence of each sample and untreated cells of each strain.

Analysis of glucose-dependent extracellular acidification

Extracellular acidification rate was estimated as previously described (Andrés et al. 2016). Briefly, after growth and treatment without or with 0-1500 µg/ml bLf or 100 µM diethylstilbestrol (DES) as reported for cell survival assays, cells were washed once with 50 mM KCl and then resuspended and concentrated (10^7 cells/ml) in 1 ml of 50 mM KCl and subjected to pH measurements. After pH stabilization, 2.5 mM glucose was added and acidification was measured every minute for 12 min using a pH meter with constant stirring. A sample was taken from each condition to estimate the dry weight after incubation at 80˚C for two days. Data is presented as ΔpH/min/mg dry weight.

Plasma membrane isolation

Plasma membranes were obtained as described previously (Andrés et al. 2016), with some modifications. Briefly, 4L of yeast culture were grown in YEPD medium until late-log phase. Cells were then harvested, washed twice with distilled sterile water and resuspended in homogenization buffer [2 mM EDTA, 2% (w/v) glucose, 1 mM phenylmethylsulfonyl fluoride (PMSF), 0.2 ng/ml DNase, 50 mM Tris pH 7.4]. Whole cells were then disrupted by three passages at 19,500 lb/in^2 in a French pressure cell (SLM Aminco, Silver Spring, MD). The resulting cell suspension was centrifuged at 3 000×*g* 4˚C for 10 min to remove cell debris and unbroken cells, and the supernatant was centrifuged twice at 14 000×*g* 4˚C for 30 min.

Afterwards, the homogenate was centrifuged at 100 000×*g* 4˚C for 1h 30 min and the pellet containing the cell membranes was resuspended in ice-cold resuspension buffer [0.5 mM EDTA, 20% (v/v) glycerol, 0.1 mM PMSF, 10 mM Tris pH=7.4]. Protein concentration was estimated by Bradford assay (Bradford 1976) before storage of samples at -80˚C.

Measurement of ATP hydrolysis

ATP hydrolysis assay was performed using the PiColorLock™ Gold Phosphate Detection kit (obtained from Innova Biosciences, Ltd. Cambridge, UK), which allows the quantification of the inorganic phosphate (Pi) concentration, according to the manufacturer's instructions. For all experiments, a calibration curve with a standard range of Pi concentrations was performed. Measurements were performed in isolated plasma membranes at a concentration of 12.5 µg/ml in assay medium containing 0.2 mM ATP. To avoid interference of the activity of vacuolar and mitochondrial ATPases and acid phosphatases, membranes were pre-incubated for 15 min at 30˚C with 50 mM KNO_3, 0.2 mM ammonium molybdate and 5 mM sodium azide (Monk et al. 1991), respectively. Afterwards, membrane extracts were incubated with 100 µg/ml bLf or 100 µM diethylstilbestrol (DES) for 15 min at 30˚C. DES was used as a positive control for Pma1p inhibition (Andrés et al. 2016). Pi concentration was calculated by spectrophotometry at 620 nm.

Evaluation of intracellular ATP concentration

Intracellular ATP concentration was quantified using the BacTiter-Glo™ Microbial Cell Viability kit as recommended. For all experiments, a calibration curve with standard ATP concentrations (10-1000 nM) was performed. Cells were grown as described for cell survival assays and treated in the absence or presence of 250 and 425 µg/ml bLf and 100 µM DES for 90 min at 30˚C with 200 rpm agitation. 50 µl of each condition were transferred to a 96-well opaque plate, mixed with equal volume of BacTiter-Glo reagent and incubated for 15 min in the dark. The emitted luminescence was read in a Varioskan flash multimode reader (Thermo Scientific). The reagent uses a thermostable luciferase that produces a luminescence signal proportional to the ATP concentration. Data is shown as arbitrary units expressed in relation to the untreated control of each strain.

Protein extraction and western blot

For preparation of whole cell extracts, 1 mL OD_{640nm}=1 of exponentially growing cells were harvested by centrifugation at 5000 ×g for 3 min and washed once with dH_2O. Cells were then

resuspended in 500 µl water containing 50 µl lysis buffer (3.5% β-mercaptoethanol in 2 M NaOH) and incubated for 15 min on ice. Next, 50 µl of 50% trichloroacetic acid were added and incubated for additional 15 min to precipitate the proteins. The extracts were centrifuged at 10 000 ×g 10 min 4˚C, washed with acetone and centrifuged again. Finally, protein extracts were resuspended in Laemmli buffer (2% β-mercaptoethanol, 0.1 M Tris pH 8.8, 20% glycerol, 0.02% bromophenol blue). Samples were heated at 95˚C and used immediately for western blot or stored at -20˚C.

For detection of Pma1p expression levels, 50 µg of protein extracts were separated by 10% sodium dodecyl sulfate-polyacrylamide gel electrophoresis for 1h. Proteins were then transferred onto nitrocellulose membranes and membranes were blocked in 5% non-fat milk in PBS-Tween 0.1% solution (1× PBST) with agitation at RT for 1 h to avoid non-specific interactions. Membranes were then cut into strips and incubated overnight at 4°C with the primary antibodies mouse monoclonal anti-yeast phosphoglycerate kinase (Pgk1p) antibody (1:5000, Molecular Probes) and mouse monoclonal antibody to Pma1p (1:1000, 40B7, Invitrogen). Pgk1p was used as the loading control. Subsequently, membranes were incubated with the secondary antibody Peroxidase-AffiniPure goat anti-mouse IgG (Jackson ImmunoResearch) (1:5000). Chemiluminescence detection was performed using the ECL detection system (Millipore-Merck) in a ChemiDoc XRS system (Bio-Rad).

Isolation of intact yeast vacuoles

Vacuole isolation was performed as previously described (Rodrigues et al. 2013; Rodrigues et al. 2018). After grown until an OD_{640} of 0.7, 1 L of BY4741 cell suspension was collected, washed twice with ice-cold distilled water, resuspended in washing buffer [5% glucose, 10 mM MES (morpholineethanesulfonic acid)-Tris, pH 6.5] and incubated in a shaker at 30°C for 30 min. Afterwards, cells were incubated with digestion buffer [1.35 M sorbitol, 10 mM citric acid, 30 mM Na_2HPO_4, 1 mM EGTA (ethylene glycol-bis(β-aminoethyl ether)-N,N,N′,N′-tetraacetic acid), 30 mM DTT (dithiothreitol), pH 7.5] for 15 min at room temperature. Spheroplasts were generated by subsequent incubation with 2 mg/mL of zymolyase in digestion buffer without DTT, and cell wall digestion was monitored in a phase contrast microscope. When digestion was completed, spheroplasts were pelleted by centrifugation at 2750 ×*g* for 5 min and washed with digestion buffer without DTT. They were then resuspended in 12% (w/v) Ficoll and homogenized in a Potter-Elvehjem to disrupt the cell membrane. To isolate vacuoles by Ficoll gradient centrifugation, the resulting homogenate

was centrifuged at 2750 ×*g* for 3 min and the supernatant was recovered. The gradient was prepared by carefully adding 8% (w/v) Ficoll on the top of the supernatant. Ultracentrifugation was performed at 80 000 ×*g* for 30 min in a SW 28 Ti swinging-bucket rotor. The white fraction on top of the gradient containing highly purified vacuoles was collected and used in the spectrofluorometric studies. Protein concentration was determined by the Lowry method (Lowry et al. 1951), using BSA (5 µg/µL - 25 µg/µL) to build the standard curve.

Measurement of V-ATPase activity by spectrofluorimetry

The pH-sensitive probe ACMA (9-amino-6-chloro-2-methoxyacridine) was used to determine the proton-pumping activity of V-ATPase in the isolated vacuoles using a Perkin-Elmer LS-5B spectrofluorimeter as previously reported (Rodrigues et al. 2013; Pereira et al. 2016; Rodrigues et al. 2018). 20 µg of isolated vacuoles were added to a buffer containing 1 mM MOPS [3-(N-morpholino)propanesulfonic acid]-Tris pH 7.2, 2 µM ACMA, 1 mM $MgCl_2$ and 100 mM KCl. The reaction was started by adding 0.1-0.5 mM ATP and the rate of initial fluorescence quenching was recorded. The excitation/emission wavelengths were set to 415 nm and 485 nm, respectively. 4 or 80 µg/ml bLf were added to the assay medium at steady-state to study their inhibitory effects. The initial rate of ACMA fluorescence quenching was considered a measure of the V-ATPase proton pumping activity [Δ%F min^{-1}] and the fluorescence quenching recovery as the inhibition of this activity. The results were analysed using the GraphPad Prism Software and the proton pumping-kinetics best fitting the experimental initial acidification curves, corresponding to the quenching of ACMA fluorescence, were determined.

Analysis of vacuolar pH variations using the carboxy-DCFDA probe

Vacuolar pH alterations were detected by both fluorescence microscopy and flow cytometry using the 5-(and-6)-carboxy-2',7'-dichlorofluorescein diacetate (carboxy-DCFDA) probe. Untreated or bLf-treated cells were harvested by centrifugation (1 mL OD_{640nm}=0.1), washed once with sterile water and resuspended in CF buffer [50 mM glycine, 10 mM NaCl, 5 mM KCl, 1 mM $MgCl_2$, 40 mM Tris, 100 mM MES pH 4.5 supplemented with 2% glucose] (Teixeira et al. 2009). The cell suspension was then incubated with 1.6 µM CDCFDA for 20 min at 30°C with 200 rpm orbital agitation. Afterwards, cells were washed once with CF buffer without glucose, and finally resuspended in the same buffer for further analysis in the flow cytometer or fluorescence microscope. Flow cytometry data are presented as the mean

FL1 fluorescence intensity in relation to the autofluorescence of each sample and untreated cells of each strain.

Immunoprecipitation **(Stéphen do you want to add a previous reference from you?)**

For immunoprecipitation, 10 ml of yeast culture at OD640=1 were collected and resuspended in a buffer containing 0.6 M Mannitol, 2 mM EGTA, 10 mM Tris/Maleate pH 6.8. Mechanic lysis was then performed using glass beads and a fast prep equipment. and supernatant was collected and centrifuged at 800 ×*g* for 10 min. 1 mg from the supernatant were solubilized in 1× IP50 buffer (Sigma-Aldrich) 40 min at 4°C and incubated overnight with 1 µg of anti-Pma1 (40B7, Invitrogen) or anti-bLf (ab112968, Abcam) antibodies. Protein G-sepharose beads (Sigma-Aldrich) were then added and incubated for additional 4 h. Beads were washed 4 times with 1× IP50 buffer and two times with 0.1× IP50 buffer, and incubated with 25 µL of Laemmli buffer 1×, before SDS-PAGE and Western-blotting.

Flow cytometry

Flow cytometry analysis was performed with an Epics® XLTM (Beckman Coulter) flow cytometer equipped with an argon-ion laser emitting a 488 nm beam at 15 mW. Green fluorescence (Carboxy-DCFDA) was collected through a 488 nm blocking filter, a 550 nm long-pass dichroic and a 525 nm band-pass filter. Red fluorescence (FUN-1) was collected through a 560 nm short-pass dichroic, a 640 nm long-pass, and another 670 nm long-pass filter. For each sample, 30 000 events were evaluated. Data were analysed using the FlowJo software.

Statistical analysis

Data are expressed as the mean and standard deviation values of at least three independent experiments. Statistical analyses were carried out using the GraphPad Prism software, one-way or two-way ANOVA and the Tukey post-test. P-values lower than 0.05 were considered to represent a significant difference.

ACKNOWLEDGMENTS

We thank Dr. Shingo Izawa and Dr. Annick Breton for the pRS316 Pma1-GFP plasmid, Dr. Amy Chang for the L3852 and XGY32 strains as well as the pAC49 AST1 plasmid, and Dr. Paula Ludovico and Dr. Belém Sampaio-Marques for the *ast1*Δ strain. This work was

financially supported by the Portuguese Foundation for Science and Technology (FCT) under the scope of the strategic funding of UIDB/04469/2020 unit and "Contrato-Programa" UIDB/ 04050/2020; and BioTecNorte operation (NORTE-01-0145-FEDER-000004) funded by the European Regional Development Fund under the scope of Norte2020 - Programa Operacional Regional do Norte; and Servicio para el Control de la Esterilización, Laboratorio de Microbiología Oral (CN-16-036). C.S.P. acknowledges the PhD fellowship PD/BD/128032/2016 funded by FCT under the scope of the doctoral programme in applied and environmental microbiology (DP_AEM).

REFERENCES

Abe F, Hiraki T. 2009. Mechanistic role of ergosterol in membrane rigidity and cycloheximide resistance in Saccharomyces cerevisiae. Biochim Biophys Acta - Biomembr [Internet]. 1788(3):743–752. http://dx.doi.org/10.1016/j.bbamem.2008.12.002

Acosta-Zaldívar M, Andrés MT, Rego A, Pereira CS, Fierro JF, Côrte-Real M. 2016. Human lactoferrin triggers a mitochondrial- and caspase-dependent regulated cell death in Saccharomyces cerevisiae. Apoptosis. 21(2):163–173.

Andrés MT, Acosta-Zaldívar M, Fierro JF. 2016. Antifungal mechanism of action of lactoferrin: Identification of H + -ATPase (P 3A -type) as a new apoptotic-cell membrane receptor. Antimicrob Agents Chemother [Internet]. 60:4206–4216. http://aac.asm.org/lookup/ doi/10.1128/AAC.03130-15

Andrés MT, Acosta-Zaldívar M, González-Seisdedos J, Fierro JF. 2019. Cytosolic acidification is the first transduction signal of lactoferrin-induced regulated cell death pathway. Int J Mol Sci. 20(23):5838.

Andrés MT, Viejo-Díaz M, Fierro JF. 2008. Human lactoferrin induces apoptosis-like cell death in Candida albicans: critical role of K+-channel-mediated K+ efflux. Antimicrob Agents Chemother. 52(11):4081–8.

Bagnat M, Chang A, Simons K. 2001. Plasma Membrane Proton ATPase Pma1p Requires Raft Association for Surface Delivery in Yeast. Mol Biol Cell [Internet]. 12(12):4129–4138. http://www.molbiolcell.org/doi/10.1091/mbc.12.12.4129

Bagnat M, Keränen S, Shevchenko Anna, Shevchenko Andrej, Simons K. 2000. Lipid rafts function in biosynthetic delivery of proteins to the cell surface in yeast. Proc Natl Acad Sci U

S A. 97(7):3254–3259.

Balguerie A, Bagnat M, Bonneu M, Aigle M, Breton AM. 2002. Rvs161p and Sphingolipids Are Required for Actin Repolarization following Salt Stress. Eukaryot Cell [Internet]. 1(6):1021–1031. https://www.ncbi.nlm.nih.gov/pmc/articles/PMC138763/

Bradford MM. 1976. A rapid and sensitive method for the quantitation of microgram quantities of protein utilizing the principle of protein-dye binding. Anal Biochem. 72:248–254.

Breton AM, Schaeffer J, Aigle M. 2001. The yeast Rvs161 and Rvs167 proteins are involved in secretory vesicles targeting the plasma membrane and in cell integrity. Yeast. 18(11):1053–1068.

Carmona-Gutierrez D, Reisenbichler A, Heimbucher P, Bauer MA, Braun RJ, Ruckenstuhl C, Büttner S, Eisenberg T, Rockenfeller P, Fröhlich KU, et al. 2011. Ceramide triggers metacaspase-independent mitochondrial cell death in yeast. Cell Cycle. 10(22):3973–3978.

Chang A, Fink GR. 1995. Targeting of the yeast plasma membrane [H+]ATPase: A novel gene AST1 prevents mislocalization of mutant ATPase to the vacuole. J Cell Biol. 128(1–2):39–49.

Cowart L, Obeid LM. 2007. Yeast Sphingolipids: Recent developments in understanding biosynthesis,. Biochim Biophys Acta. 1771(3):233–245.

Daicho K, Makino N, Hiraki T, Ueno M, Uritani M, Abe F, Ushimaru T. 2009. Sorting defects of the tryptophan permease Tat2 in an erg2 yeast mutant. FEMS Microbiol Lett. 298(2):218–227.

Dechant R, Binda M, Lee SS, Pelet S, Winderickx J, Peter M. 2010. Cytosolic pH is a second messenger for glucose and regulates the PKA pathway through V-ATPase. EMBO J [Internet]. 29(15):2515–2526. http://dx.doi.org/10.1038/emboj.2010.138

Eggleston MD, Marshall PA. 2007. Saccharomyces cerevisiae samples stained with FUN-1 dye can be stored at -20°C for later observation. J Microsc. 225(1):100–103.

Estrada AF, Muruganandam G, Prescianotto-Baschong C, Spang A. 2015. The ArfGAP2/3 Glo3 and ergosterol collaborate in transport of a subset of cargoes. Biol Open. 4(7):792–802.

Farnoud AM, Mor V, Singh A, Del Poeta M. 2014. Inositol Phosphosphingolipid

Phospholipase C1 Regulates Plasma Membrane ATPase (Pma1) Stability in Cryptococcus neoformans. FEBS Lett. 588(21):3932–8.

Fernandes KE, Carter DA. 2017. The antifungal activity of lactoferrin and its derived peptides: Mechanisms of action and synergy with drugs against fungal pathogens. Front Microbiol. 8:1–10.

Fernandes KE, Weeks K, Carter DA. 2020. Lactoferrin is broadly active against yeasts and highly synergistic with amphotericin B. Antimicrob Agents Chemother. 64(5):1–22.

Gaber RF, Copple DM, Kennedy BK, Vidal M, Bard M. 1989. The yeast gene ERG6 is required for normal membrane function but is not essential for biosynthesis of the cell-cycle-sparking sterol. Mol Cell Biol [Internet]. 9(8):3447–3456. http://mcb.asm.org/lookup/doi/10.1128/MCB.9.8.3447

Gaigg B, Timischl B, Corbino L, Schneiter R. 2005. Synthesis of sphingolipids with very long chain fatty acids but not ergosterol is required for routing of newly synthesized plasma membrane ATPase to the cell surface of yeast. J Biol Chem. 280(23):22515–22522.

Gietz RD, Woods RA. 2006. Yeast Transformation by the LiAc/SS Carrier DNA/PEG Method. In: Methods Mol Biol - Yeast Protoc Second Ed [Internet]. Vol. 313. [place unknown]; p. 107–120. http://www.springerprotocols.com/Abstract/doi/10.1385/1-59259-958-3:107

Gong X, Chang A. 2001. A mutant plasma membrane ATPase, Pma1-10, is defective in stability at the yeast cell surface. Proc Natl Acad Sci [Internet]. 98(16):9104–9109. http://www.pnas.org/cgi/doi/10.1073/pnas.161282998

Grossmann G, Malinsky J, Stahlschmidt W, Loibl M, Weig-Meckl I, Frommer WB, Opekarová M, Tanner W. 2008. Plasma membrane microdomains regulate turnover of transport proteins in yeast. J Cell Biol. 183(6):1075–1088.

Guedes J, Pereira C, Rodrigues L, Côrte-real M. 2018. Bovine milk lactoferrin selectively kills highly metastatic prostate cancer PC-3 and osteosarcoma MG-63 cells in vitro. Front Oncol [Internet]. 8(200):1–12. http://doi.org/10.3389/fonc.2018.00200

Guillas I, Kirchman PA, Chuard R, Pfefferli M, Jiang JC, Jazwinski SM, Conzelmann A. 2001. C26-CoA-dependent ceramide synthesis of Saccharomyces cerevisiae is operated by Lag1p and Lac1p. EMBO J. 20(11):2655–2665.

Hao L, Shan Q, Wei J, Ma F, Sun P. 2019. Lactoferrin: Major Physiological Functions and Applications. Curr Protein Pept Sci. 20(2):139–144.

Kane P. 2016. Proton Transport and pH Control in Fungi. Adv Exp Med Biol. 892:33–68.

Kinoshita T, Fujita M. 2016. Biosynthesis of GPI-anchored proteins: special emphasis on GPI lipid remodeling. J Lipid Res [Internet]. 57(1):6–24. http://www.jlr.org/lookup/doi/10.1194/jlr.R063313

Kitagaki H, Cowart LA, Matmati N, Vaena de Avalos S, Novgorodov SA, Zeidan YH, Bielawski J, Obeid LM, Hannun YA. 2007. Isc1 regulates sphingolipid metabolism in yeast mitochondria. Biochim Biophys Acta - Biomembr. 1768(11):2849–2861.

Kodedová M, Valachovič M, Csáky Z, Sychrová H. 2019. Variations in yeast plasma-membrane lipid composition affect killing activity of three families of insect antifungal peptides. Cell Microbiol. 21(12).

Kuipers ME, De Vries HG, Eikelboom MC, Meijer DKF, Swart PJ. 1999. Synergistic fungistatic effects of lactoferrin in combination with antifungal drugs against clinical Candida isolates. Antimicrob Agents Chemother. 43(11):2635–2641.

Lahoz E, Pisacane A, Iannaccone M, Palumbo D, Capparelli R. 2008. Fungistatic activity of iron-free bovin lactoferrin against several fungal plant pathogens and antagonists. Nat Prod Res. 22(11):955–961.

Lee MCS, Hamamoto S, Schekman R. 2002. Ceramide biosynthesis is required for the formation of the oligomeric H+-ATPase Pma1p in the yeast endoplasmic reticulum. J Biol Chem. 277(25):22395–22401.

Lowry OH, Rosebrough NJ, Farr L, Randall RJ. 1951. Protein Measurement with the Folin Phenol Reagent. J Biol Chem. 193(265–275).

Martinez-Montanes F, Lone MA, Hsu FF, Schneiter R. 2016. Accumulation of long-chain bases in yeast promotes their conversion to a long-chain base vinyl ether. J Lipid Res [Internet]. 57(11):2040–2050. http://www.jlr.org/content/57/11/2040.full.pdf

Maxfield FR, Wüstner D. 2012. Analysis of Cholesterol Trafficking with Fluorescent Probes. Methods Cell Biol. 108(1):367–393.

Millard P, Roth B, Thi H-G, Yue S, Haugland R. 1997. Development of the FUN-1 Family of

Fluorescent Probes for Vacuole Labeling and Viability Testing of Yeasts. Appl Environ Microbiol [Internet]. 63(7):2897–2905. http://ovidsp.ovid.com/ovidweb.cgi?T=JS&PAGE=reference&D=med1&NEWS=N&AN=159705

Mollinedo F. 2012. Lipid raft involvement in yeast cell growth and death. Front Oncol [Internet]. 2(140):1–15. http://journal.frontiersin.org/article/10.3389/fonc.2012.00140/abstract

Monk BC, Kurtz MB, Marrinan JA, Perlin DS. 1991. Cloning and characterization of the plasma membrane H+-ATPase from Candida albicans. J Bacteriol. 173(21):6826–6836.

Moreno-Expósito L, Illescas-Montes R, Melguizo-Rodríguez L, Ruiz C, Ramos-Torrecillas J, de Luna-Bertos E. 2018. Multifunctional capacity and therapeutic potential of lactoferrin. Life Sci [Internet]. 195:61–64. https://doi.org/10.1016/j.lfs.2018.01.002

Munn AL, Heese-Peck A, Stevenson BJ, Pichler H, Riezman H. 1999. Specific Sterols Required for the Internalization Step of Endocytosis in Yeast. Mol Biol Cell [Internet]. 10(11):3943–3957. http://www.molbiolcell.org/doi/10.1091/mbc.10.11.3943

Pacheco A, Azevedo F, Rego A, Santos J, Chaves SR, Côrte-Real M, Sousa MJ. 2013. C2-phytoceramide perturbs lipid rafts and cell integrity in Saccharomyces cerevisiae in a sterol-dependent manner. PLoS One. 8(9):1–12.

Pan J, Hu C, Yu JH. 2018. Lipid biosynthesis as an antifungal target. J Fungi. 4(2):1–13.

Pasrija R, Prasad T, Prasad R. 2005. Membrane raft lipid constituents affect drug susceptibilities of Candida albicans. Biochem Soc Trans. 33(5):1219–1223.

Pereira CS, Guedes JP, Gonçalves M, Loureiro L, Castro L, Gerós H, Rodrigues LR, Côrte-real M. 2016. Lactoferrin selectively triggers apoptosis in highly metastatic breast cancer cells through inhibition of plasmalemmal V-H+-ATPase. Oncotarget [Internet]. 7(38):62144–62158. http://doi.org/10.18632/oncotarget.11394

Pierce A, Colavizza D, Benaissa M, Maes P, Tartar A, Montreuil J, Spik G. 1991. Molecular cloning and sequence analysis of bovine lactotransferrin. Eur J Biochem [Internet]. 196(1):177–84. http://www.ncbi.nlm.nih.gov/pubmed/2001696

Pina-Vaz C, Sansonetty F, Rodrigues AG, Costa-Oliveira S, Tavares C, Martinez-De-Oliveira J. 2001. Cytometric approach for a rapid evaluation of susceptibility of Candida strains to antifungals. Clin Microbiol Infect [Internet]. 7(11):609–618. http://dx.doi.org/10.1046/j.1198-743x.2001.00307.x

Prudêncio C, Sansonetty F, Côrte-Real M. 1998. Flow cytometric assessment of cell structural and functional changes induced by acetic acid in the yeasts Zygosaccharomyces bailii and Saccharomyces cerevisiae. Cytometry. 31(4):307–313.

Rautenbach M, Troskie AM, Vosloo JA. 2016. Antifungal peptides: To be or not to be membrane active. Biochimie [Internet]. 130:132–145. http://dx.doi.org/10.1016/j.biochi.2016.05.013

Roberts C, Raymond C, Yamashiro C, Stevens TH. 1991. Methods for studying the yeast vacuole. Methods Enzymol. 194:644–661.

Rodrigues J, Silva RD, Noronha H, Pedras A, Gerós H, Côrte-Real M. 2013. Flow cytometry as a novel tool for structural and functional characterization of isolated yeast vacuoles. Microbiology. 159:848–56.

Rodrigues JMP, Pereira CS, Fontes N, Gerós H, Côrte-Real M. 2018. Flow Cytometry and Fluorescence Microscopy as Tools from Yeast and Plant Cells. Plant Vacuolar Traffick Methods Protoc. 1789:101–115.

Sawai H, Okamoto Y, Luberto C, Mao C, Bielawska A, Domae N, Hannun YA. 2000. Identification of ISC1 (YERO19w) as inositol phosphosphingolipid phospholipase C in Saccharomyces cerevisiae. J Biol Chem. 275(50):39793–39798.

Schorling S, Vallée B, Barz WP, Riezman H, Oesterhelt D. 2001. Lag1p and Lac1p Are Essential for the Acyl-CoA–dependent Ceramide Synthase Reaction in *Saccharomyces cerevisae*. Mol Biol Cell [Internet]. 12(11):3417–3427. http://www.molbiolcell.org/doi/10.1091/mbc.12.11.3417

Siafakas AR, Wright LC, Sorrell TC, Djordjevic JT. 2006. Lipid rafts in Cryptococcus neoformans concentrate the virulence determinants phospholipase B1 and Cu/Zn superoxide dismutase. Eukaryot Cell. 5(3):488–498.

Sorensen M, Sorensen S. 1939. The proteins in whey. Compte rendu des Trav du Lab Carlsb. 23(7):55–99.

Staubach S, Hanisch F-G. 2011. Lipid rafts: signaling and sorting platforms of cells and their roles in cancer. Expert Rev Proteomics. 8(2):263–77.

Steijns JM, van Hooijdonk ACM. 2000. Occurrence, structure, biochemical properties and technological characteristics of lactoferrin. Br J Nutr. 84(S1):11–17.

Teixeira MC, Raposo LR, Mira NP, Lourenço AB, Sá-Correia I. 2009. Genome-wide identification of Saccharomyces cerevisiae genes required for maximal tolerance to ethanol. Appl Environ Microbiol. 75(18):5761–5772.

Toulmay A, Schneiter R. 2007. Lipid-dependent surface transport of the proton pumping ATPase: A model to study plasma membrane biogenesis in yeast. Biochimie. 89(2):249–254.

Umebayashi K, Nakano A. 2003. Ergosterol is required for targeting of tryptophan permease to the yeast plasma membrane. J Cell Biol. 161(6):1117–1131.

Wang Q, Chang A. 2002. Sphingoid base synthesis is required for oligomerization and cell surface stability of the yeast plasma membrane ATPase, Pma1. Proc Natl Acad Sci U S A [Internet]. 99(20):12853–12858. http://www.ncbi.nlm.nih.gov/entrez/query.fcgi?cmd=Retrieve&db=PubMed&dopt=Citation&list_uids=12244215

Zaremberg V, Gajate C, Cacharro LM, Mollinedo F, McMaster CR. 2005. Cytotoxicity of an anti-cancer lysophospholipid through selective modification of lipid raft composition. J Biol Chem. 280(45):38047–38058.

Zhang YQ, Gamarra S, Garcia-Effron G, Park S, Perlin DS, Rao R. 2010. Requirement for ergosterol in V-ATPase function underlies antifungal activity of azole drugs. PLoS Pathog. 6(6):e1000939.

Figure S1 - Exogenous addition of C2-ceramide sensitizes cells to bLf and rescues the resistance phenotype of the *lac1*Δ strain

Since *LAC1* encodes a component of ceramide synthase, the enzyme involved in the *de novo* synthesis of ceramide, we investigated the effect of exposing wild type and *lac1*Δ cells to exogenous addition of N-Acetyl-D-sphingosine (C2-ceramide), a membrane-permeable form of ceramide. For that purpose, and since C2-ceramide was found to induce cell death in yeast (Carmona-Gutierrez et al. 2011), we chose a non-toxic dose of this agent for both strains. The combined exposure of cells to bLf and C2-ceramide yielded a significantly higher sensitivity than the individual exposure to each compound in both strains. Notably, the resistance phenotype of the *lac1*Δ mutant is completely rescued by addition of

C2-ceramide and the mutant cells become even more sensitive than wild type cells treated only with bLf. The addition of C2-ceramide also greatly enhanced the sensitivity of wild type cells to bLf.

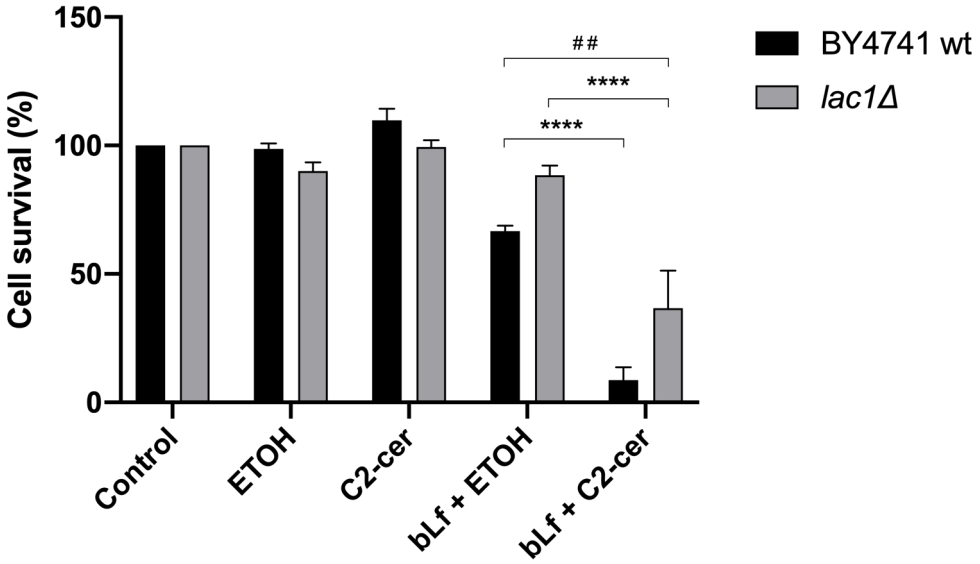

Figure S1 | Effect of bLf and C2-ceramide on cell survival of wild type and *lac1*Δ mutant strains. (A) Cell survival assays of *S. cerevisiae* BY4741 wild type and *lac1*Δ mutant strains after 90 min of incubation at 30˚C with 50 µg/ml bLf and/or 20 µM C2-ceramide (C2-cer) in 10 mM Tris-HCl buffer pH 7.4, evaluated by colony forming unit counting. Absolute ethanol (ETOH) is the C2-cer solvent. Values are mean ± standard deviation normalized to time zero of incubation and considering the control without bLf as 100% cell survival. **** $P<0.0001$ between the indicated conditions in the same strain; ## $P<0.01$ between the indicated conditions of different strains.